Chapter-IV

Channel Behaviour and Pattern

4.1 Introduction

Channel behavior is related with the existing channel processes that lead to frequent changes in the water and sediment flow pattern of the river. River patterns express an additional mechanism of channel adjustment which is related to channel gradient and cross-section (Leopold et al., 1964). It changes with hydro-morphological changes of the basin. Flow resistance within the channel causes large changes in the channel pattern. The channel geometry is linked up with basin plan-form; sub-surface structure, basin erosion; channel gradient and vegetation cover etc. The first order drainage connectivity collectively directs the upper catchment run-off to the higher order streams. The spacing of the first order drainage branches below the rugged terrain of *Pankhasari* ridge (400 m) creates the head of the basin. The dendritic pattern merges into the narrow channels of *Kali* and *Chel* which flows downstream in a structurally controlled river course. The channel behaviors reflects its tendency of auto-cyclic cut and fill process related with recent base level changes. The morphogenesis of the channel evolves with the changes of the relative heights of the existing river terraces. The rate of channel incision along the base of higher terraces forms narrow gorges for the channel flow. The hilly segment of the course is influenced by the extension of ridges and higher terraces. The orogenetic movements of the recent past have its influence on the channel. The 5^{th} order channel of *Chel* becomes visible near *Ambiok* tea garden. After that, it shows high sinuous course with the sign of boulder deposits and diverted course. The valley on the right side of the channel is broader beside *Gorubathan Khasmahal*. At the mountain outlet, the course has been turned to S-E to fall on the fan surface. It flows almost parallel to the curved upper *Fagu* ridge. The extension of the *Gorubathan* fault controls the sharp turn of the river channel here. Above the mountain outlet, the channel shows high flow efficiency with boulder bed formation. The channel starts braiding below *Ambiok* tea garden. The narrow channel wanders between *Dalingma* and *Fagu* ridge. The existence of slightly vegetated channel bars indicates the stability of the course. The phases of flash floods modify the position of the channel bars. The mechanism of heavy bank failure supplies coarse bank materials to the channel. The high channel

competency distributes the large boulder up to the mountain outlet. After that it converts into an alluvial channel with fine sand deposits.

Channel behavior changes frequently downstream due to the supply of discharge as related with the gradual decrease in the slope. The pattern of channel bar formation is related with the supply of sediment from the up-stream. So, the basin erosivity and sediment yield processes are important to exaggerate the tendency of bar formations. On the piedmont surface, the channel hydraulic geometry transforms by the supply of high amount of bed load and the recession of peak flood discharge settles the suspended load in the channel. In the sedimentary environment at fan surface, the anticipated flow finds several sub-surface conduits to flow downstream. The mid part of the fan diverts the main channel towards their banks. The bank walls face high shear stress against the rampant flow during monsoon. The process of bank failure supplies high amount of sediment load to the discharge. The heavy sediment load creeps down the channel bottom against the existing channel force exceeding the threshold of inertia of the sediment particle. The lighter sediment particles having less weight than the buoyant force experience an upward flux of eddy momentum by the capacitate discharge along the channel boundary. During heavy discharge, the increased flux of suspended load decreases the fluid stress component by reducing the magnitude of oscillation of turbulences (Leopold et al., 1964). This process is effective in the stabilization of the channel bars. The suspended load entrainment in the channel is dependent on the channel force times the settling velocity of the fluid. This suspended load settles down the bed when the amount of discharge recedes quickly to the downstream. The formation of grain layers within the flowing discharge is created by the dispersive grain stress which directs upward against the normal gravitational pulling (Bagnold, 1954 and Leopold et al., 1963). This fluid stress constructs the height of the channel bars. The formation of channel bars leads to the diversion of the flow towards the bed and banks. The morphology of the alluvial fan surface dissipates the flow energy of load transportation and creates favorable condition for aggradation. The channel load movement is dependent on the two opposite shear stresses acting variably on channel bed and on fluid to exceed the threshold for movement. Channel behavior is well connected with its discharge, pattern of bar formation, channel boundary condition, sediment load movement and type of the channel load.

4.2 Methodology

4.2.1 The morphology of channel bars, shape of multi-thread channel and tendency braiding have been analyzed and calculated by following the methods of Braiding index (Brice, 1964), Sinuosity Index (Muller, 1968, Morisawa, 1985, Brice, 1964).

4.2.2 The site-wise (Upper *Fagu*, *Patharjhora* and *Manabari* tea garden) nature of channel bar formation has been studied from Google Earth images (2016 & 2017) and also cross-verified with field observations.

4.2.3 The nature of channel avulsion has been studied from the thorough analysis of temporal Google earth images (1983, 1990, 2007 & 2016) at the same scale and same UTM (Universal Transverse Mercators) projection layout. The process and type of channel avulsion has been carried out by following the classification of Jones (2007). The intensive sites of avulsion (beside *Patharjhora* tea garden, below *Patharjhora* tea garden and beside west *Damdim* TG) have been studied from Google earth images and also by attempting fields.

4.2.4 The nature and rate of course shifting have been analyzed from satellite images (Landsat 3 MSS, Landsat 5 TM-30 m, Landsat 6 ETM & Landsat 8 OLI-TIRS) (1970, 1990, 2000 & 2019) and Google Earth images (1981, 2001 & 2016) by drawing nine successive cross-sections along the river at an interval of 3 km. The shifting tendency of river banks and its width variations have been computed from the same temporal scale.

4.3 Channel behaviour and fan morphology

Pattern of Channel Plan form Dynamics (CPD) has linked a variety of flow conditions and sediment regimes actually those which are seriously controlled by climatic and geologic conditions (Brierley, 2010 & Cheng-Wei, 2017). The dominant channel pattern is haphazard anabranching streams with properties of sinuosity, braiding and sediment load characters (Mollard, 1973 & Rust, 1978) that illustrate the hydrological and channel morphological evolutions. As per Rouse 1965 Flow resistance within the channel actually causes changes in the channel load pattern which is of four types as per componential aspects: (a) surface resistance, (b) form resistance, (c) wave resistance from free suface effects, and (d) resistance due to local acceleration mainly

through flow unsteadiness (Järvelä, 2004) which is more evident here. Manning's "n" value for roughness due to bed bottom irregularity shows moderate to high resistance ranging between 0.03~0.05 (average 0.04). At the mountain, the course has been turned to South-East to fall on the fan surface. It flows almost parallel to the curved upper Fagu ridge. Dating of Radiocarbon signatures of organic rich clay components indicate the *Gorubathan* thrust post-dated to 33,875± 550 Ka BP (Bansal et al., 2013) and is still active (Guha et al. 2007) and having imprints of surface ruptures. Though dynamism can be attested with gravels from 5 m depth near *Ranichera* tea garden (lower terrace) associated with 30m high terrace of River Chel (Starkel et al., 2015) which is showing Optically-Stimulated Luminescence dating (OSL) of 57.4 ± 4.4 ka (kilo annum: 1000 yr. span) BP (Before present) meaning thereby about 59,600 year old than 1950 or 0 BPY and the fan surface is dissected by the younger rivers emanating out from the mountainous foreland. The migrating Himalayan front tectonically cross-cut these fans and tilting, folding and uplifting is quite common (Srivastava, 2017).The identified contour segments unshadows the scenario that Fan Face Morphology (FFM) is reshaped by huge load depositions due to loss of surface drainage and wastage of runoff in an area having more than 1,000-1,500 mm per annum of rainfall. The areal segments bounded by contours viz. 200-220m, 240-260m, 260-280m and 280-300 m are accounting for gradient of 1 in 1074.01,1 in 84.45,1 in 51.85 and 1 in 43.75 almost low to negligible low gradient initiated by frequent avulsion and anabranching drainage pattern implicating on the outer fan face and factorized through equilibrium vs. in-equilibrium of explained sediment transport capacity as well as channel sedimentation processes. The struggle of the channel to transport load with feeble velocity has repercussion on changing channel shape (w/d: Channel width-depth ratio) and multi threading of channel with anabranching and high channel roughness (Nanson, 1999).

4.4 Observation on present channel form

Carson and Griffiths (1987) recognized some types of braided rivers: like unstable multiple stream, stable multiple stream, and multi-thalweg stream which is noticeable in case of Chel being mostly unstable multiple type. Both the erosional and depositional fluvial characteristics are responsible for complex braiding. Ashmore in 1991 identified four types of mechanisms of braid formation viz. middle bar accretion

(MBA), transverse bar conversion (TBC), chute cut-offs (CCO), and multiple bar dissection (MBD) out of which MBD is quite common here. Chute cut-off is visible along the course of *Manzing Khola* (Fig. 4.1).

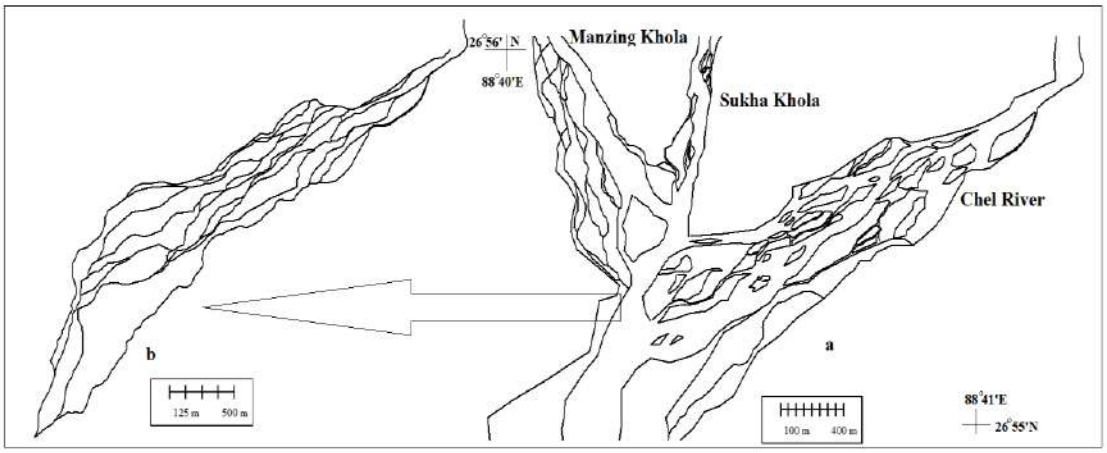

Figure 4.1 Present braided channel network of Chel; a. Braid network at tri junction point above Patharjhora tea garden, b. 2018 extracted (Google Earth) multi-thread course of Chel on piedmont surface.

The mid-channel accretion bars inclusively Linguoid types [Lepold et al., 1957] have elongated downstream direction and is observable beside *Manabari* TG (Fig. 4.4) and West *Damdim*. The identical mid channel gravel bars composed of lag sediment deposits are predominant beside *Patharjhora* TG (Fig. 4.3). The presence of transverse bars [Ashmore, 1991] and their ongoing transformation process significantly indicates the dominance of comparatively good stream power condition at *Gorubathan* site (Fig. 4.2).

4.4.1 Reach 1 (Beside Upper Fagu ridge)

This site is confined between *Mal* and upper *Fagu* ridge (Fig. 4.2).The channel widens gradually to the right bank. The average width of the reach is 164 m and the length of the reach is 1 km. The channel sinuosity value is 1.12. The flow is directed to the left bank. The point bars have been developed at the right bank. The flow along the inner point bars creates chutes by scouring at one side. Later on, this incipient point bar converts into medial bar. Three prominent medial gravel bars have been formed at the flow paths. One mid channel vegetated bar is also identifiable. The transverse bar along the left bank converts into an elongated medial bar as the flow alters around it.

4.4.2 Reach 2 (Beside Pathrjhora tea garden)

The channel becomes wider after reaching at the piedmont surface (Fig. 4.3). The average channel width beside *Patharjhora* tea garden is 1.15 km. This is because of the sudden decrease of the channel gradient (1 in 52 m) at the mountain outlet. The flow diverges towards the channel boundary after being retarded by mid channel bars. During the pre-monsoon season, only the flow is found to active along the right bank of the channel. The bed form is composed of pebbles and sand deposition. The finer sediment size varies from 19-91 mm. But, some flood driven boulders of 50 cm to 90 cm are also observed on the channel bed. The pattern of bar formation is complex is this site. Because, the piedmont surface is highly imperceptible of any strong flow pattern on it. The situation is favorable for high dissipation of channel energy. After the passage of monsoon, the variable bed forms raise up from the submerged condition.

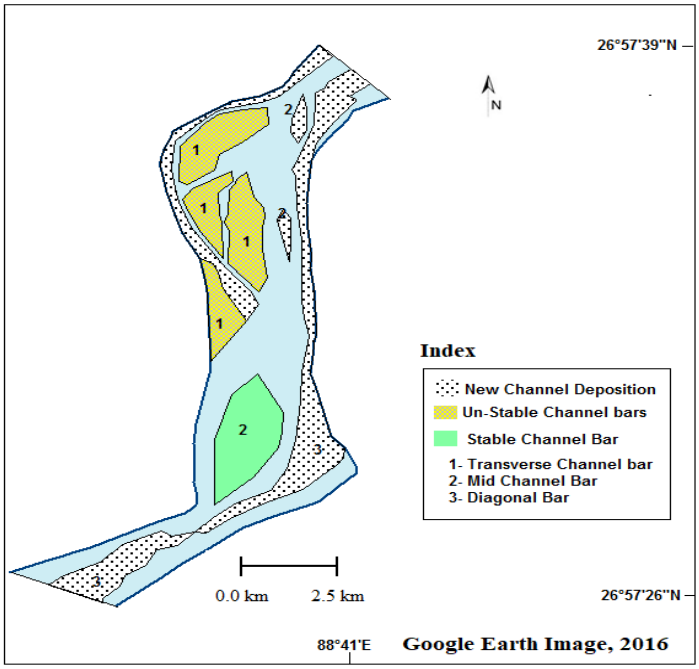

Figure 4.2 Channel bar formation and pattern beside Gorubathan.

The cyclic process of channel filling becomes stronger at the same point before the end of one flood cycle. The right bank tributaries of the Chel are observed to compose of chute cut bar formations along the right banks. The chute related bar diversion is attributed by the formation of sudden flood channel along the banks. The main channel of Chel is composed by the formation of an elongated mid channel bar close to the right bank. This bar has been developed since last two flood cycle events.

The tow of this bar is attached with a transverse bar wants to spread out to the banks. This led to the diversion of channel to the banks near *Patharjhora* site. The channel deposition alters with every monsoonal discharge. The mid channel bars shits downstream depending on the flow velocity. The presence of channel scours is observable at the front of the medial bars.

4.4.3 Reach 3 (Beside Manabari tea garden)

This site carries the evidence of channel oscillation on the lower extension of the fan surface (Fig. 4.4). The channel has been shifted towards west and increases the occurrences of bank erosion along the right bank. The site is natural without any embankment that leads to promote the occasional bank slips to the west. The main channel is infested by sediment load and reveals high braided pattern of flow. The channel widths are very narrow and flowing by dissecting the sediment bed.

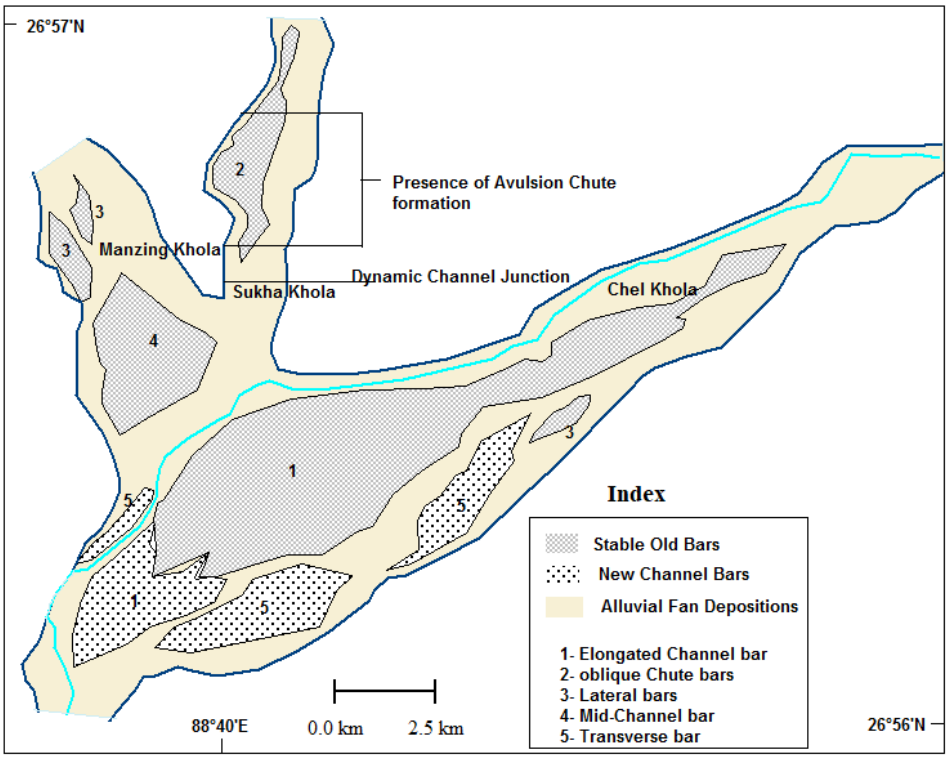

Figure 4.3 Channel bar formation and pattern beside Patharjhora.

The pattern has been formed due to the obstacle created by the sediment bed. The site is dominated by the formation of elongated point bars. The channel is carrying numerous mid channel bars. These bars are newly formed by previous flood deposition. The height of the bars is highly variable as their formation is influenced

by the seasonal variable discharge. The main active channel exists along the right bank. The immediate lower part of the site does not carry such braided pattern due to the existence of an embankment along the right bank. This site also carries the sign of channel avulsion. Many small streamlets become activated on the flood plain to the east and these channels are mainly reoccupied channels. The upper part of the reach also expresses braided tendency and avulsion. The channel avulsed towards the *Lethi khola* through various small reoccupied streamlets.

4.5 Channel Avulsion: temporal analysis

The term is synonymous with the switching of flow from one channel to another (Ferguson, 1993). The process of avulsion is related with the higher rate of sedimentation in the channel that cause the diversion of the previous flow paths in to new path to flush out the accumulate sediment. The main cause of avulsion is related with shifting of the existing course in to new course and blocking of channels by the bars (Charlton, 2008). The avulsion process of a channel is also linked with the duration and peakedness of triggering flood, ratio of sediment flux in discharge, geometry of the avulsion node and pre-existing topography of the flood-plain.

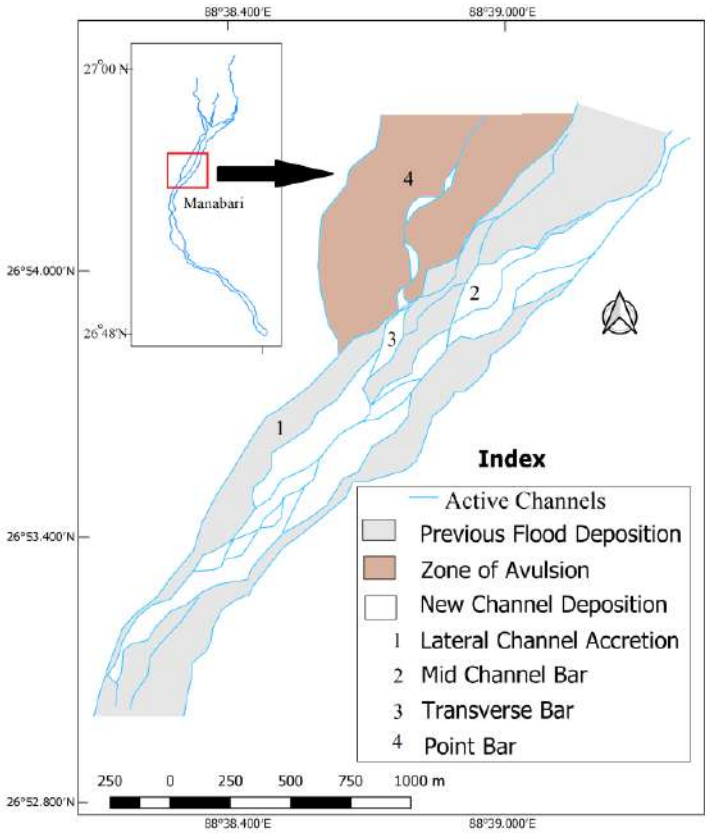

Figure 4.4 Channel bar formation and pattern beside Manabari.

The process indicates the rapid transfer of river flow from the established channel belt. Avulsion is a dominant depositional mechanism. Avulsion means the sudden abandonment of a part or the whole of a meander belt by a stream for some new course at a lower level on the floodplain (Allen, 1965). It causes new braiding pattern within the existing channel (Nanson and Knighton, 1996). It also states the diversion of flow from an existing channel onto the floodplain, eventually resulting in a new channel belt (Makaske, 2001). The shifting of the previous course in to new set up can cause the dispersal of sediment load present in the discharge. This phenomenon can only be measured up by considering in large spatio-temporal scale. The channel gradient factor and basin erosivity are typically attributed in causing channel avulsion. The channel avulsion is not only related with the channel abandonment as well it re-occupies the old channels on the flood plain. The stratigraphic analysis of avulsion can be considered from transitional and abrupt process of deposition (Jones et al., 2007).

4.5.1 Present and Past Conditions of Channel Avulsion

Avulsion is not only the process of excessive sediment diversion to a newly formed channel rather it controls the distribution of coarse and fine grained deposits in a channel. It functions through the ongoing fluvial process of the channel. The loss of channel gradient on the piedmont surface leads to the formation of aggrading channel beds. The submerged channels in the sedimentary environment create a complex connectivity of continuous sediment and water flow by the process of annexation (Fig. 4.5). Avulsion by annexation occurs when an avulsed channel reoccupies an abandoned channel or appropriates an existing channel (Jones, 2007). The vibrant course of Chel has been affected by multi-cyclic processes of fluvial action. So, it shifts abruptly on the piedmont surface supported by the appearance on floods. The bank deposits in horizontal strata and their tier wise arrangement indicate the two or many different active phases of flood events. The channel fill deposits and bank deposits are the key to find the early phases of fluvial deposits and the channel morphological adjustment of avulsion. The rate of avulsion has been exaggerated by the blocking channel bars. The river Chel has formed many new bypasses on the foreland basin to remove the increasing sediment load within the old channel sediment belt and thus exhibits anastomosing avulsion process. The channel bars

shifts the course near the banks. During the high flow, the channel spreads out on the floodplain and starts deposition on the soft alluvium in form of crevasse splays. Avulsion is related with the water and sediment diversion via crevasses splays on the flood-plain. The splay formations are the courses of narrow water flow paths where the channel levee become breached out during high water stage. The avulsed channel directly incises the previous channel deposits and the avulsed channel becomes stratigraphically abrupt (Jones, 2007). The braided morphology of the channel at the outlet is highly unstable because of variable discharge from the upper catchment. The channel abandons one active flow path along its right bank near *Patharjhora*.

4.5.1.1 Avulsion at Site 1(Beside Patharjhora)

The site is situated on the piedmont tract of Darjeeling Himalaya at an elevation of 320 m (Fig. 4.7).The length of the site along the course of Chel is 3.2 km. The site is a junction of three stream connectivity namely Chel, Fagu and Manzing khola. The site is identical with its variable discharge, sedimentary environment and high stream energy dissipation. The width of the flood plain beside *Patharjhora* TG is 1.5 km. The maximum channel width is 800 meter. This wide channel is composed of various blocking channel bars. The channel widens out on the fan surface. The right bank of Manzing khola gives the birth of many narrow streamlets in form of a complex network of connectivity. This avulsion process follows annexation of previous channels by new channels. Avulsion by annexation occurs when an avulsed channel re-occupies an abandoned channel or appropriates an existing channel (Jones, 2007). The process of avulsion is limited on the adjacent flood plain. The left bank of Chel reveals the same process of avulsion. The existence of those under-fit channels are only feed by the monsoon water. This site bears the imprint of aggradational avulsion process (Fig. 4.7). As aggradational or progradational avulsion is characterized by an early stage of deposition and multi-channel distributaries develop as the parent channel loses an increasing amount of flow and sediment to newly developed channel (Jones, 2007). The joining of three streams on the fan surface leads to the accumulation of sediment. The width-depth ratio of the reach becomes high. The channel incision during monsoon discharge is observed to confine near the banks. The channel spreads out on the fan surface due to the effective dispersion of sediment load by the recurring events of flash floods (1963, 1968, 1993, 1996, 2000, 2016, and

2017). The role of flash floods when overtops the banks initiates the overland flow on the margins of the fan surface. This overland flow generates various ephemeral streamlets on the fan margins. The course of these small active channels cuts down on the previous alluvium of fan surface. These on-fan streams involve in the process of active head ward erosion that leads to back migration of the apex of the fan. The rate of back filling by the small channels causes further aggradation of the channel. Overland flow is more likely to result in a channel avulsion if a nearby channel is receiving the flow (John, 2000).

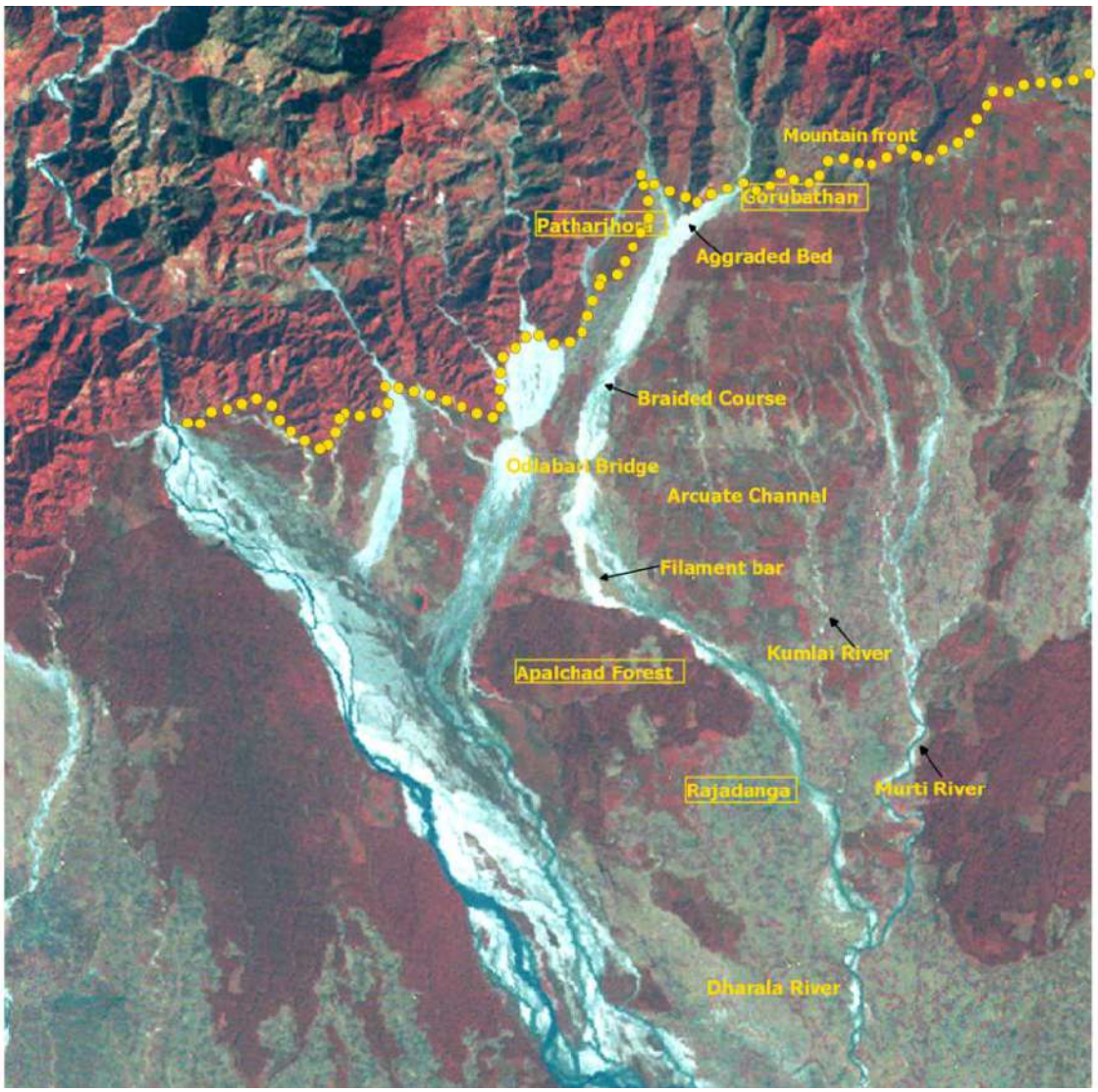

Figure 4.5 False colour composite of MSS bands (1970) showing sediment infested upper course of Chel (above *Odlabari* bridge) and arcuate shaped channel form with increasing sinuosity in lower part (below *Odlabari* bridge).

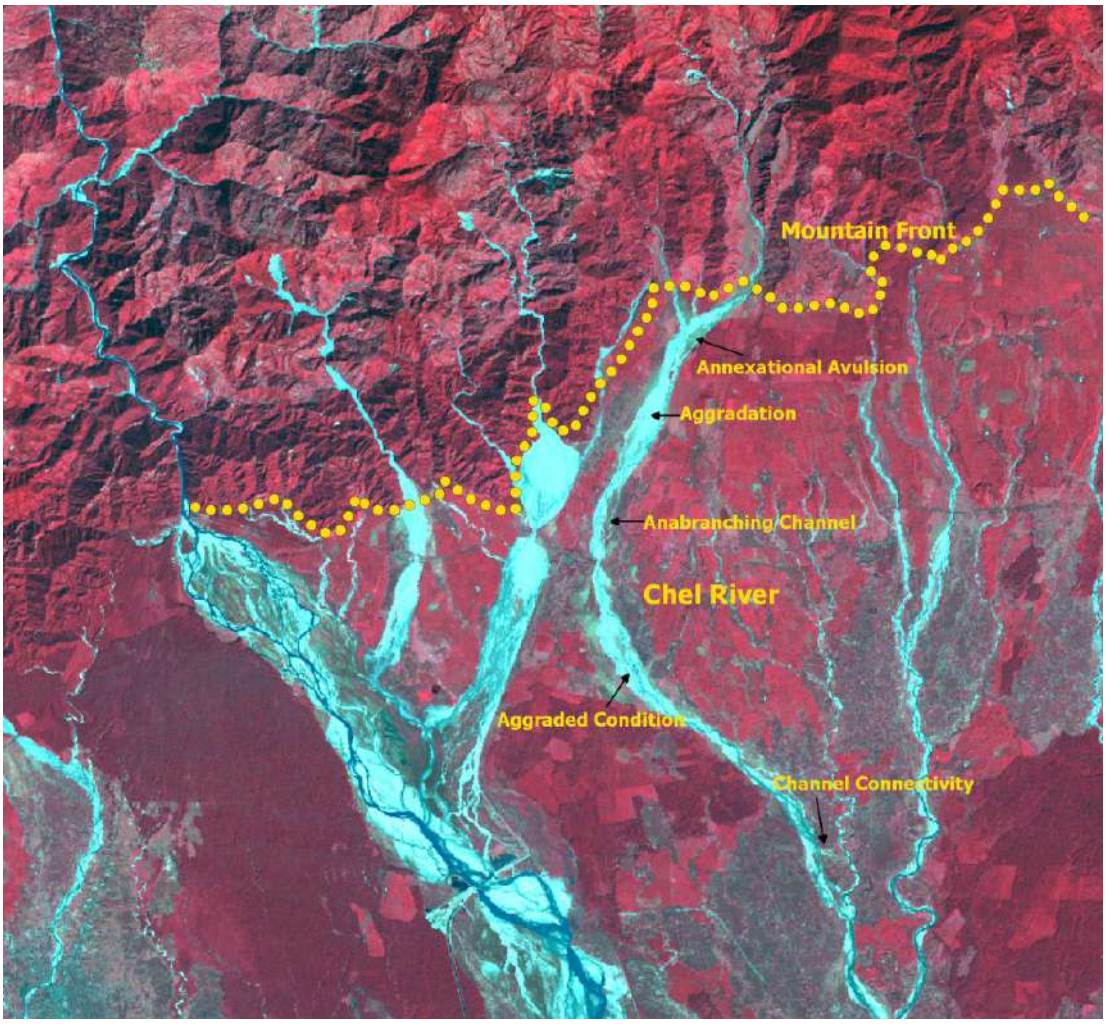

Figure 4.6 False colour composite of TM bands (1990) showing the process of annexational avulsion at Patharjhora, massive bed aggradation at Manabari, Avulsion through anabranches at Turibari and dynamics channel confluence of Kumlai river.

The present channel of Chel is highly susceptible by means of aggradational avulsion process. The amount of sediment discharge is highly variable at the piedmont tract. The connecting streams are supplying high amount of sediment load to the main course of Chel. The right bank of Manzing khola starts developing anabranches which directly establish connectivity with the right bank of Chel beside *Patharjhora*. The *Manzing khola* migrates to the west with many channel diversions. The measured width of the course along with the branches is 500 m. Above *Patharjhora*; the channel of *Manzing Khola* divides in to two different channels by the blocking effect of a medial channel bar. It expresses a chute diversion pattern of avulsion as it is observed from the satellite image of 2016 (Fig. 4.10 c). The type of avulsion by the blocking effect of channel bars is the dominant process of this site.

The Channel of Chel is diverted by a large medial bar on the fan surface beside Mal forest and it comes close to the left bank. This left bank of Chel is the surface of sheet flood occurrences (Fig. 4.7). It leads to the continuous channel widening.

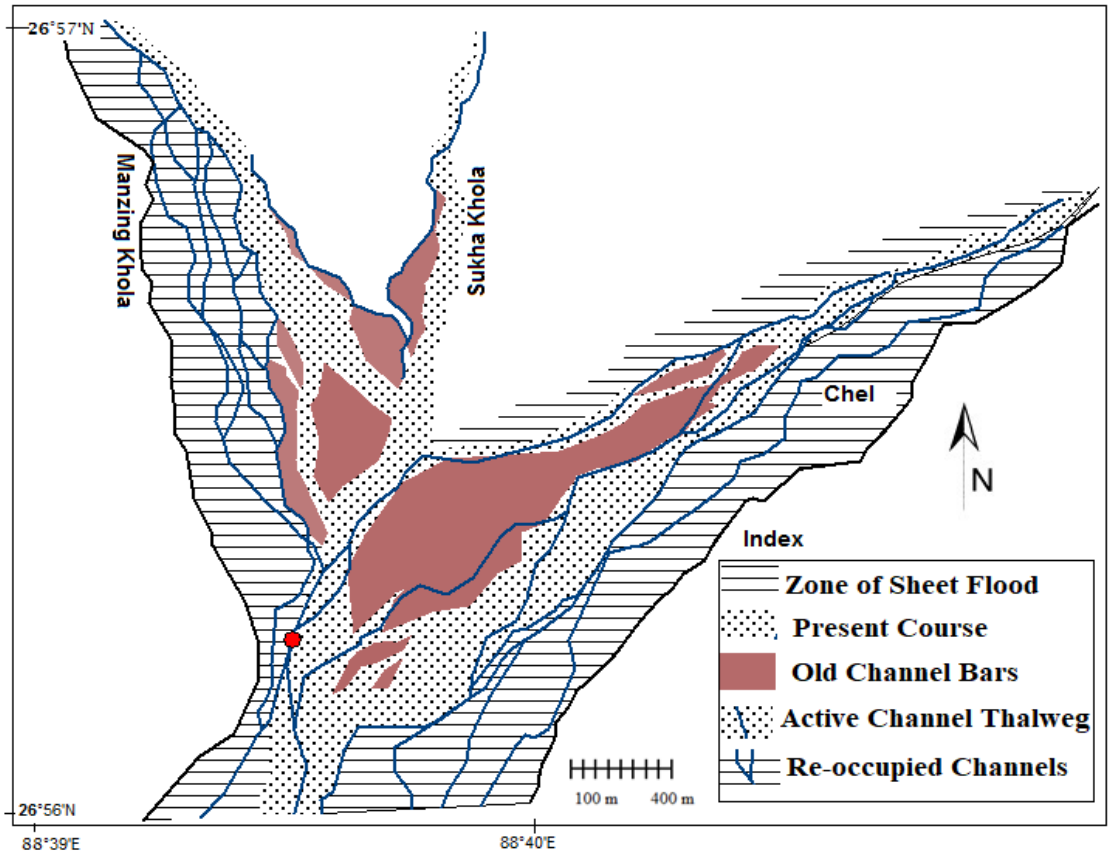

Figure 4.7 Present condition of channel avulsion beside Patharjhora.

At *Patharjhora* site, the maximum channel width is 640 m. The main flow path of Chel has continuously been shifted to the west. The active left anabranch of the channel is completely vanished in the image of 2016. Anabranches of some braided channels appear to be near the threshold condition of equilibrium (Leopold et al, 1964). The present course of Chel (640 m) becomes wider than the previous course of 2007 (380 m). Above *Patharjhora*, the two channels of *Manzing* and *Fagu khola* creates a junction. The left bank of *Manzing khola* directly connects with the course of *Sukha Khola*. The Channel of *Sukha khola* becomes prominent along the left bank and the beheaded part of the channel becomes under fit within the valley. The channel creates a new chute branch along its right bank (2016 image). From 2007 to 2016, the main course of Chel has expressed abrupt changes in the channel form and pattern. The flash flood events before 2016 affected the channel pattern and converted it in to

a braided stream. This multi-thread channel accumulates new sediment along the channel bars. The avulsion process runs by the blocking effect of channel bars. The channel of 2016 is composed by large a medial bar which is not visible in the image of 2007. This new stable bar is composed of comparatively old alluvium and stays above the water height of recent flood occurrences. The activity of right bank flow path is still active because of the combined supply water and sediment at the V-junction and through the left anabranch of *Manzing khola*.

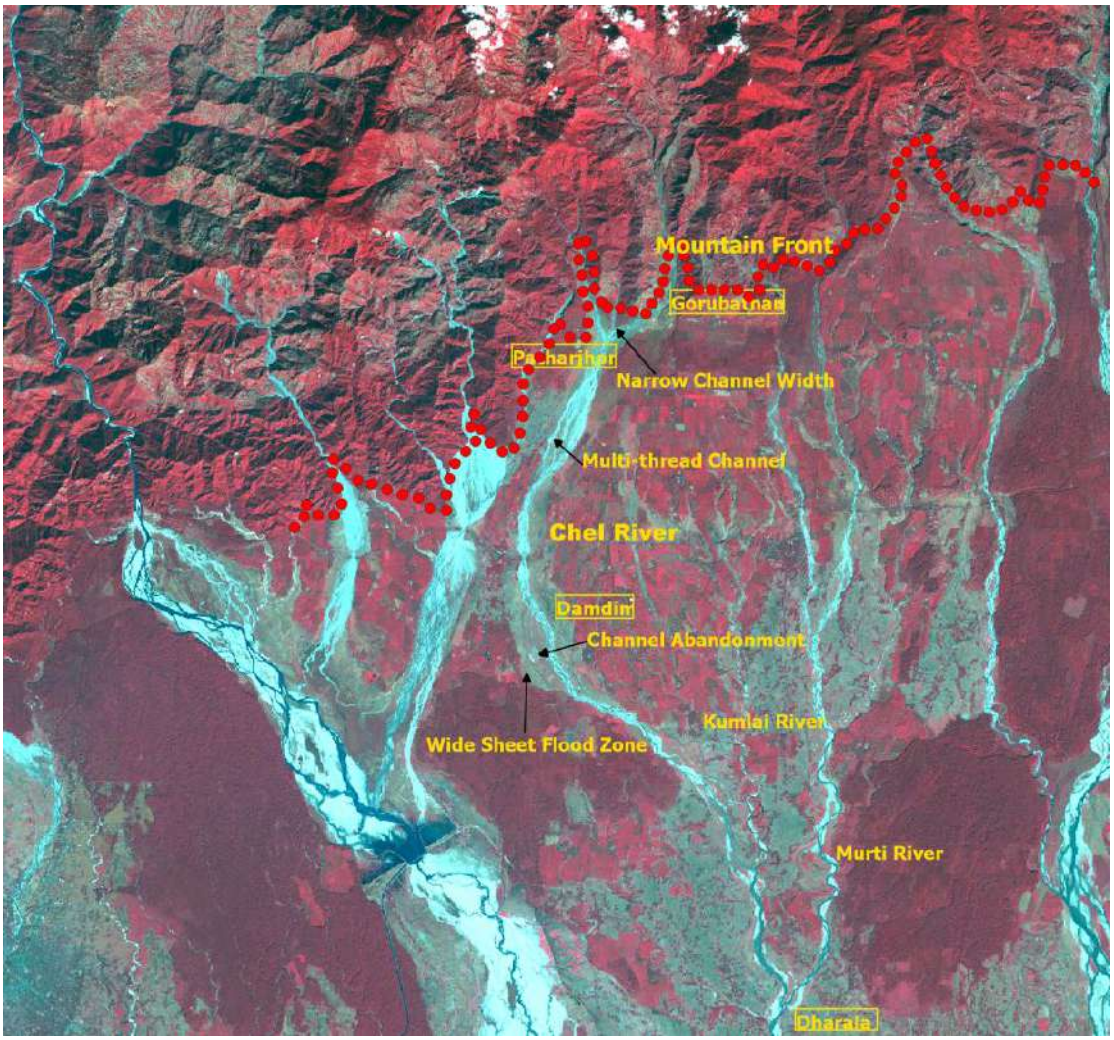

Figure 4.8 False colour composite of ETM bands (2000) showing high channel transformation (channel narrowing at tri-junction point, below Odlabari bridge, channel anastomosing at Manabari, channel abandonment at right bank at Damdim & change in the arcuate shape below Odlabari bridge) after the passage of serial extreme rainfall events (1993, 1996, 2000).

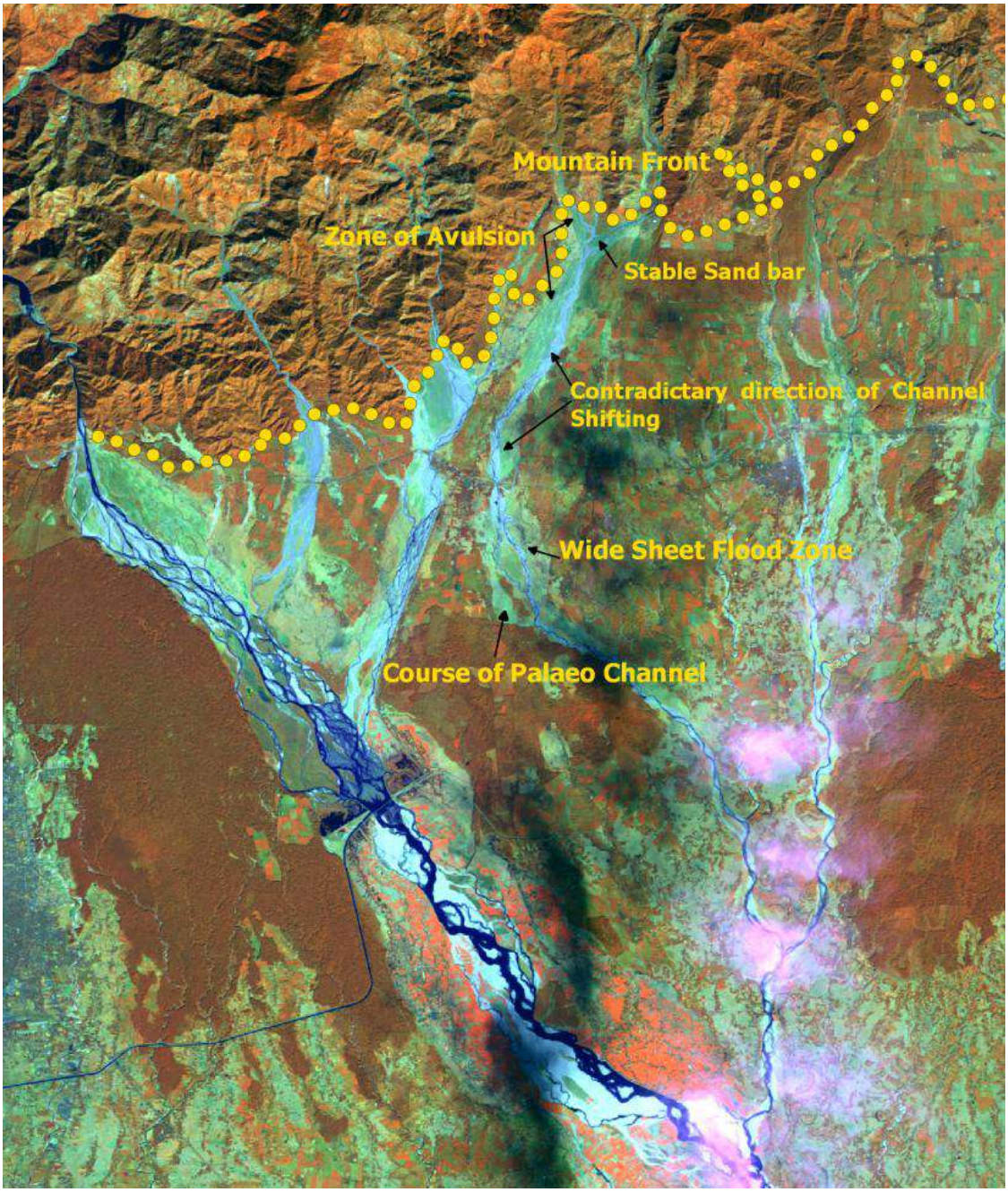

Figure 4.9False colour composite of OLI-TIRS (Landsat 8) bands (2019) showingcontracdictary direction of channel shifting at Manabari and Turibari, zone of avulsion vis-à-vis sheet flood appears along the right bank near Patharjhora, below the Odlabari bridge course of Chel diverts along a large stable filament shaped bar.

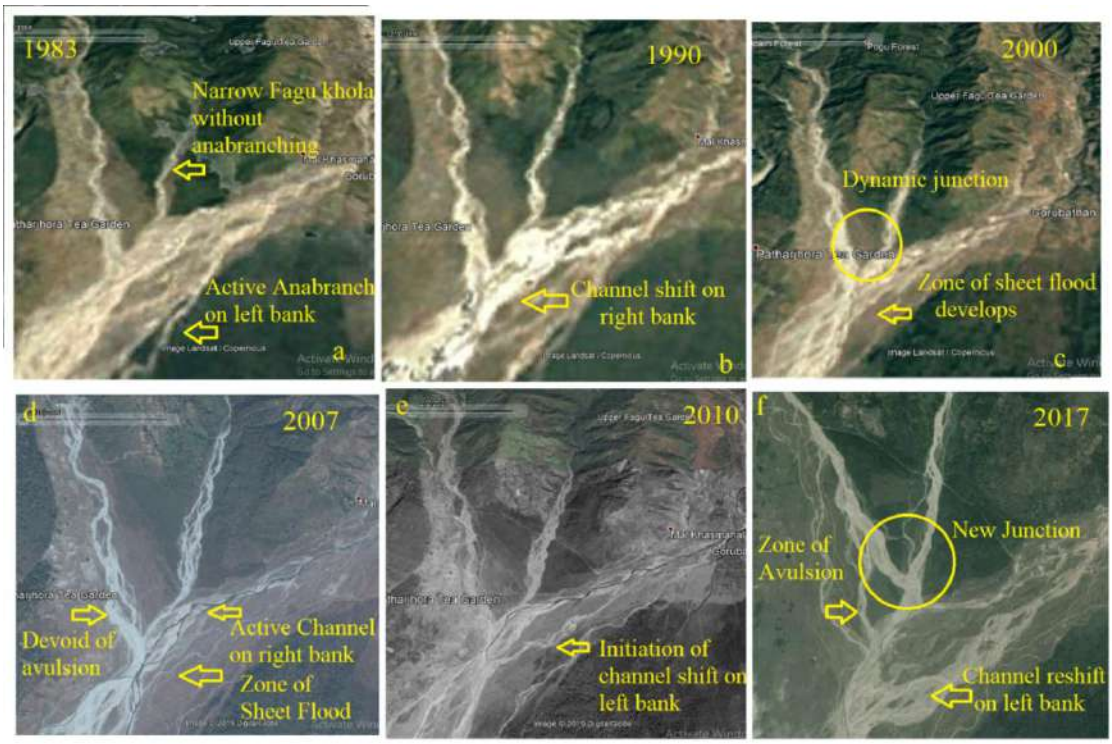

Figure 4.10 Temporal conditions of channel avulsion at Patharjhora: a. Old channel shifts regularly on right bank leaving imprint of active channel anabranch, b. Channel becomes more active on right bank leaving a wide zone of sheet flood, c. Channel widens and starts developing avulsion channels on sheet flood zone (left bank), d. Active channel of Chel flows near the left bank, the sheet-flood zone becomes wide, stream junction is absent, anastomosing pattern of Fagu khola, e. Channel starts re-shifts on left bank with channel bar diversion, through anabranching and avulsion f. Recent avulsion site beside Patharjhora where flow diversion by the medial bar occupies a larger area on the sheet flood zone, Manzing and Fagu Khola get connected, Many anabranches develop on the right bank of Manzing khola.

The course of Chel in 1983 (Fig. 4.10 a) expresses a continuous sedimentary channel without any diversion. The channel width is calculated as 850 m. A channel branch is observed along the left bank and this branch is also observable in the image of 1990. The course of *Fagu khola* and *Manzing khola* was observed as narrow in the image of 1983. But both the channel becomes wider in the image of 1990. The channel width gradually narrows down to 830 m in 1990. From 1983 to 2007, the channel of Chel expressed a tendency to migrate towards west. But in 2016 it again comes back to the east due to avulsion. Presently, the multi-thread course of Chel indicates high rate of avulsion (Fig.4.10 f).The development of incipient channel bars and sediment yield from upper catchment is mainly responsible for such avulsion.

4.5.1.2 Avulsion Site 2 (Below Patharjhora)

The present process of avulsion follows the formation of newly created anabranches along the right bank of the channel. The process is related with massive sediment infestation of the channel beside *Turibari* tea garden. From the satellite image of 2016, it reveals the pattern of annexation where the top of the channel spreads at the downstream from an apex (Fig. 4.11 a).

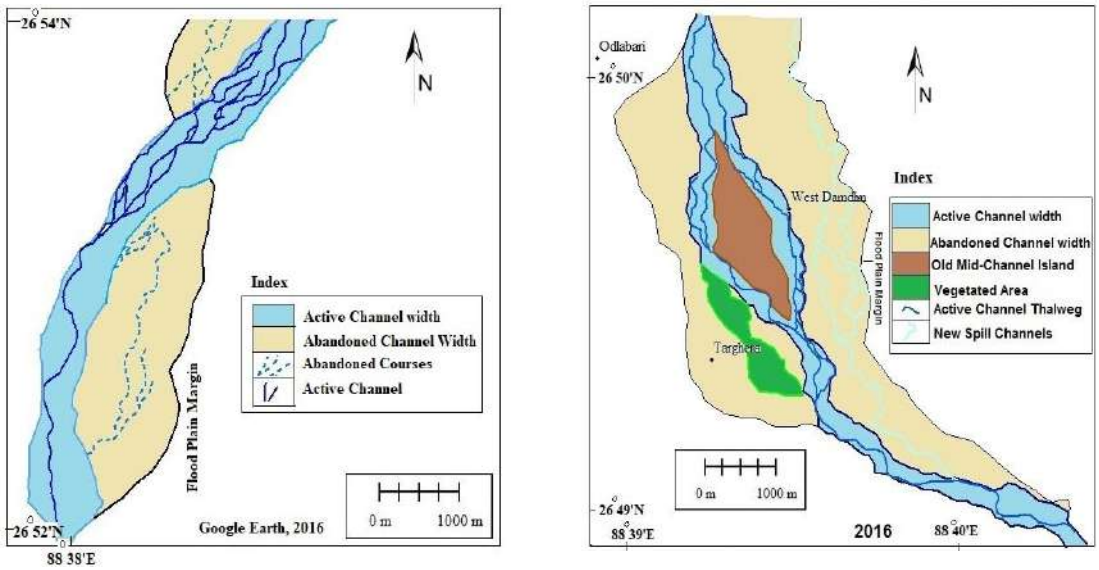

a **b**

Figure 4.11 Present Condition of channel Avulsion: a. Avulsion mapping beside Manabari b. Avulsion mapping beside Damdim.

The movement of sediment load with monsoon discharge is observed to competent at this site. The course gradually shifts to the east. The channel is fully devoid of the formation of sediment bars. But, the channel in 2006 represents a channel diversion by the positional effect of an elongated stable mid channel bar (Fig. 4.11 a). The channel pattern was to the vicinity of ideal braiding. In 2002, the channel of Chel (1.12 km) was narrow than 2006 (670 m).The flow was diverted into three channels and divided by the position of three stable mid channel bars. The right anabranch appeared as a strong part of the channel. The process reveals the annexation type of avulsion. This type of local avulsion (Slingerland et al., 2004) creates various new channels that rejoin the main channel at down-stream. The two diverted channels on the right bank of Chel in 2002 get merged into a single channel in 2006 (Fig. 4.12 c). In 2016, the active anabranches in the single channel belt has been formed by the re-occupation of channel along left bank.

Figure 4.12 Dynamic behaviour of channel pattern with the signs of avulsion (Turibari & Manabari): a. Appearance of new anabranches along the right bank, b. Channel diversion by a large elongated mid channel bar, c. Appearance of three active channels, d. Continuous channel with single Mid-channel Island, e. Sediment infested channel without braiding, f. Highly braided course along the left bank, g. Appearance of short anabranch, h. Appearance of a long anabranch along the left bank.

Another stretch of 5 km has been considered to analysis the tendency of channel avulsion. The process of avulsion is dominated by the abandonment of an anabranch on the left bank of the channel (image of 1990). A new shorter connection has been established on the left bank in 1996. The beheaded part of the previous connection (1990) had been died out due to the relocation of the anabranch (Fig. 4.10 d). The channel width had also been reduced from 450 m to 430 m in 1996 after the relocation. A distributary channel has been noticed below the *Manabari* tea garden in 1996 (Fig: 4.12 c). The channel is completely absent in the images of 2006 and 2016. The image of 2006 reveals the tendency of gradual west-ward shift of the main channel. It lefts a 600 m zone of paleo flow channels on the left bank of the channel (Fig: 4.12 f). This zone indicates the previous channel belt and still receives new flood depositions.

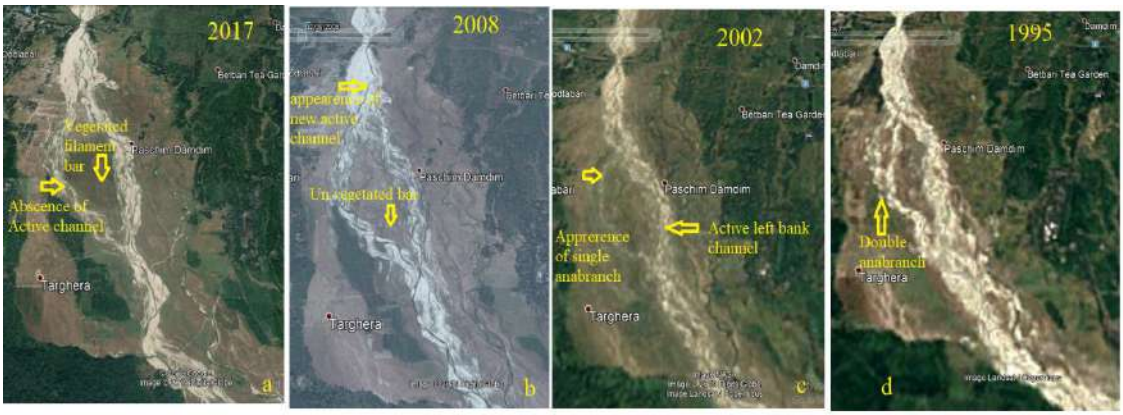

Figure 4.13 Temporal change in channel behaviour: a. Inactivation of right channel diversion and stabilization of the filament mid channel bar b. Multi thalweg course of Chel with re-occupied channel on the right bank, c. Abandonment of the anabranch along the right bank of Chel, d. Double connected anabranch on the right diversion of the channel.

4.5.1.3 Avulsion Site 3 (Beside West Damdim)

Below the *Odlabari* bridge site, the channel takes a sharp bend to the South-East. The present course of Chel (2017) creates a filament beside west *Damdim* (Fig. 4.13 a). The channel divides to avoid the blocking effect of a stable mid-channel bar (Fig. 4.11 b). The course was more braided in 2008. At this site, the present width of the channel belt is measures as 2.5 km. This wide zone experiences number of channel abandonment and re-occupation from 1988. The shape of the channel has been continuously changing since 1988. The noticeable fact of changes in this site is pivoted on the continuous changes of the width of channel flood belt. The channel of 1988 is observed as continuous and sediment infested without any sign of channel avulsion. The channel divides in to two parts in the image of 1995 (Fig. 4.13 d). The branch of the channel becomes narrower on the right bank in the image of 2002 (Fig. 4.13 c). Again the channel becomes prominent on the right side division in 2004. The existence of the vegetated patch of land on the right bank beside *Targhera* indicates the stability of the course and less extreme event of channel over spilling. The repeated events of channel over spilling at local sites of the channel bank cause the activation of avulsion (Slingerland et al., 2004). The active spill channels attribute the main channel along the left bank and thus make it vulnerable for spilling of monsoonal discharge. The process is dominated by the high accumulation of sediment below the bridge site and it slow transportation to the downstream. The pressure of sediment load causes the diversion of the channel. The equal diversion at the apex of

the blocking mid channels bar causes the re-activation of the right bank channel. The increasing channel sinuosity causes high bank stress at the outer side of the bend. Although, the root binding effect of the trees of *Apalchad* forest protects it to form full meander (Fig. 4.13 a).

4.6 Changes in the channel

The shifting of a channel is associated with the variable sediment load discharge in the channel. The variability of channel shifting is also attached with the seasonal flood frequencies that initiate the process of heavy bank wasting on the piedmont tract of Darjeeling Himalaya. The frequent changes in stage of erosion contribute to the instability of the transport regime and to the mechanism of bank erosion (Leopold et al., 1964). The composition of the bank of *Chel Khola* is dominated by coarse unconsolidated sediments. The bank wasting process follows over toppling of lose bank materials in the main channel. This process also exaggerated the phenomena of bed aggradation. The aggradation of the channel bed further causes the diversion of flow to the banks. At *Patharjhora* site, the flow is only alive along the banks of the channel and it involves in rapid channel incision especially during the monsoon. The measured height of the right bank at *Patharjhora* site is 5 m. This amount of incision is done by at least previous five flood phases. The asymmetric cross-section of the channel is due to the un-equal rate of bank erosion on both sides. The position of the channel bars plays a key role in the uneven distribution of stream power at the reach.

4.6.1 Condition of channel in 1964

The course of Chel on the piedmont surface exhibits a tendency of rapid sedimentation due to decline in channel gradient from 25 per thousand to 15 per thousand within a streatch of 10 km. Beside *Patharjhora* tea garden, the valley widens up to 1.75 km after receiving two small rivers namely *Sukha khola* and *Manzing Khola*. Below Upper *Fagu* tea garden, the channel of Chel expresses high sinuosity with sedimentation without any indentical bar formation. The course of Chel follows WNW-ESE oriented falut line below the *Gorubathan* ridge (Starkel, 2008). The fan surface starts below the *Gorubathan* ridge where the lower erosional terrace surface (15 to 20 m) merges with the active fan head. The main course of Chel is observed at the right margin of the active fan surface, actually tried to laterally spread towards the *Patharjhora* tea garden. The process of channel avulsion was dominant

along the right bank where *Manzing* and *Sukha* khola merges. The flow of *Manzing* khola from *Danbar basti* to the tri-junction shows expansion along the right bank.The maximum width of *Manzing khola* is measured 613 m above the tri-junction. The *Chel khola* starts expandind below *Sombaria* market of *Gorubathan* and the left bank moves towards *Mal basti* (east). The measured channel width is 391 m beside *Mal basti*. Beside *Patharjhora* tea garden, the channel forms a wide alluvium deposition belt whose head is found to be connected below Upper *Fagu* ridge. The channel is infested with small fragmented mid channel bars with vegetation cover (Fig. 4.14 b). In 1964, the presence of dense *Sakkam* forest slows down the process of channel avulsion along the left bank. The width of the channel retained above 1 km up to *Turibari*. From *Turibari* to *Odlabari* rail bridge, the channel compresses by width and retained braided behaviour with fragmented mid channel bars. The existence of multi-thread channel is observed very prominent beside *Manabari*. At *Odlabari* bridge, the channel width is measured only 108 m. From this site, the channel start starts facing high anthropogenic pressure.

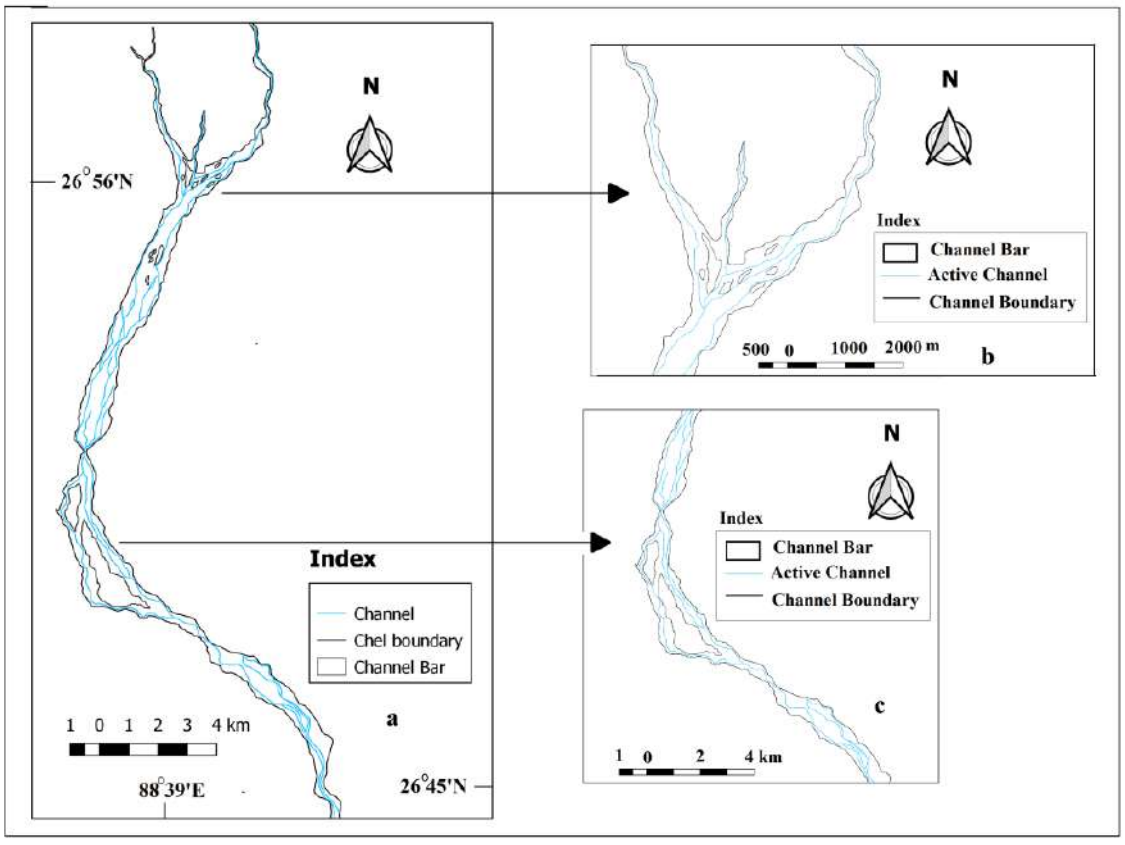

Figure 4.14 Course of Chel in 1964 (SOI Topographical map); a. Old course of Chel, b. Course on piedmont & c. Course on alluvial plain.

Below *Odlabri* bridge, the channel again starts increasing by width. The channel width is measured as 800 m beside *Bengbari* basti. Below *Damdim*, the channel starts flowing around inhabited islands like *Targhera* and *Hanskhali* settlements (Fig. 4.14 c). The presence of *Apalchad* reserve forest diverts the channel to S-E and the channel takes the sharp bend with increasing channel sinuosity. Near *Rajadanga*, the course of Chel finally merges with its left bank tributary *Kumlai*.

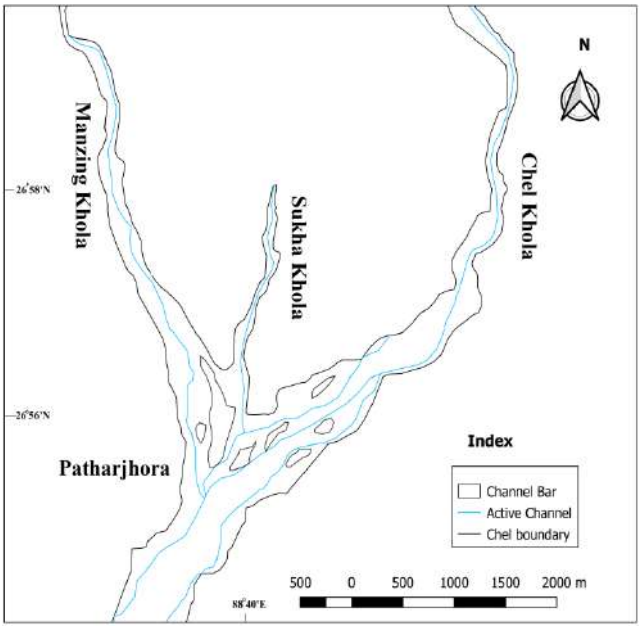

Figure 4.14b Semi braided course of Chel with fragmented mid channel bars.

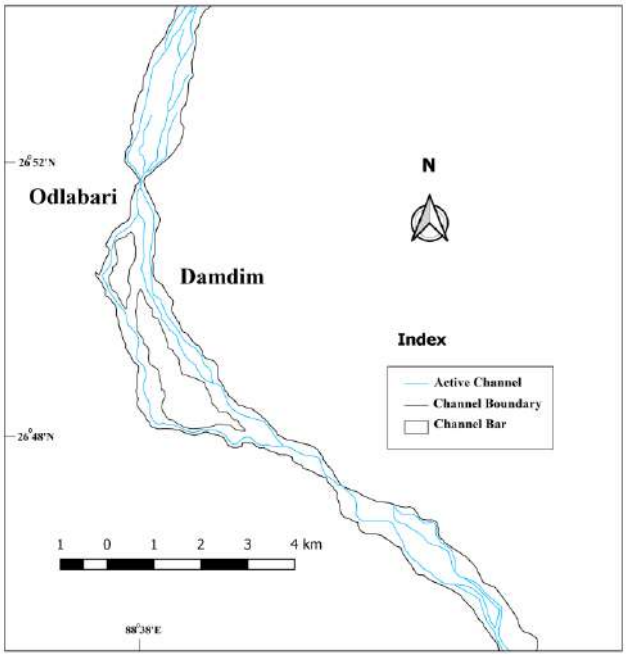

Figure 4.14c Multi-thread course of Chel with stable filament shaped mid channel bar below Odlabari bridge.

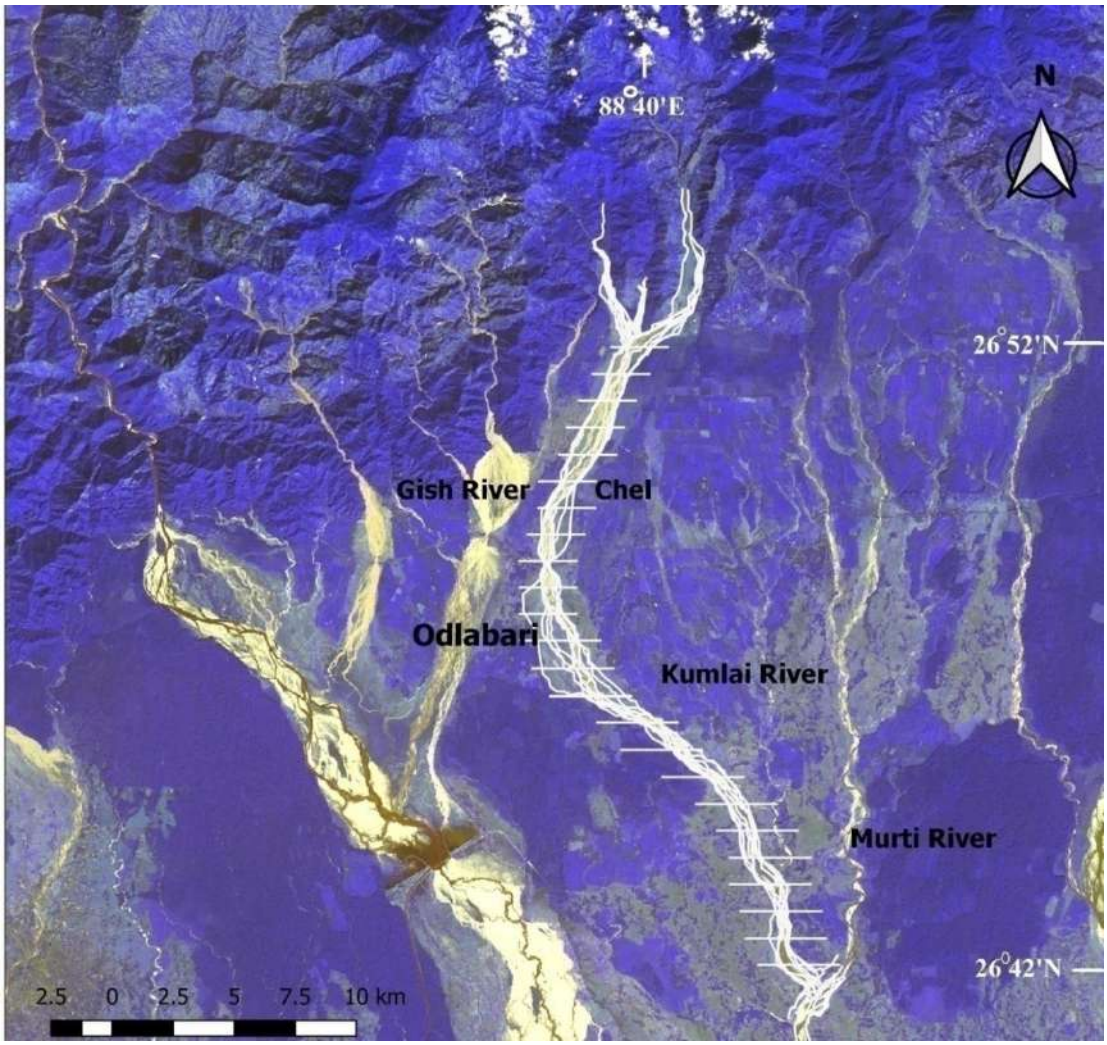

Figure 4.15 Cross sections for course shifting analysis (1970 to 2019).

4.6.2 Course Shifting of Chel: a temporal analysis

The analysis of the rate of course shifting has been done by drawing successive cross-sectional lines along at an interval of 1 km to the downstream and total 24 cross-sections have been taken across the course (Fig. 4.15). In each cross-section, the changes in left and right bank have been measured. The respective channel widths have also been measured. The change in the bank lines is not observed to proceed in the same direction rather it oscillates. The directional changes of the banks are also observed (Fig. 4.16 b & c). But, the channel width decreases sharply from 1970 to 2019 and the average decrease in channel width is measured as 517 m in 49 years (Fig. 4.17). So, the average rate of channel decrease is further calculated as 10.55 m year^{-1}. The maximum chages in width has been observed at site 13 (below *Damdim*) and 14 (*Apalchad*) as 1981 m and 1014 m (40.4 m year^{-1} and 20.69 m year^{-1}). The

decrease in channel width is connected with decreasing rain storm events after 2007, channel mining, construction of channel embankment and the bridge at *Odlabri*. Only except near *Rajadanga* (site 22), the channel width increases slightly (24 m in 49 years). Beside *Patharjhora* (site 1), the rate of channel width change is measured as 8.04 m year^{-1}. The identical change above (222 m) and below (633 m) *Odlabari* bridge in 49 years (1970 to 2019) is quite significant to notice. This change is the result of embankment construction above and below the bridge during different times. The maximum change in left bank has been calculated for site 13 (beside *Damdim*) as 1361 m and maximum change in right bank is 786 m at site 11 (below *Odlabari* bridge).

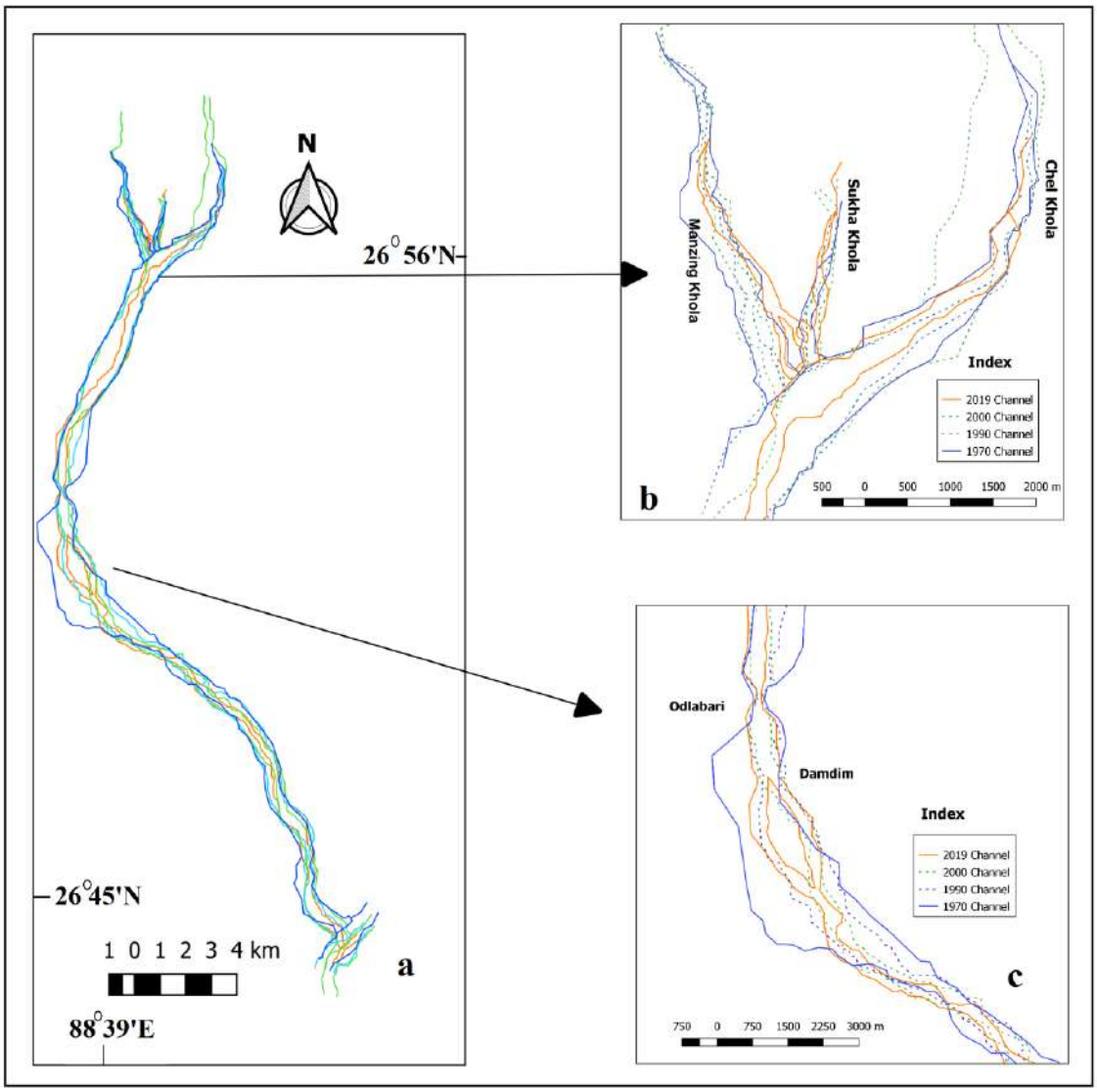

Figure 4.16 Course shifting analysis; a. Temporal analysis of course shifting, b. Course shiting at piedmont (beside Patharjhora) and c. Course shifting below Odlabari bridge.

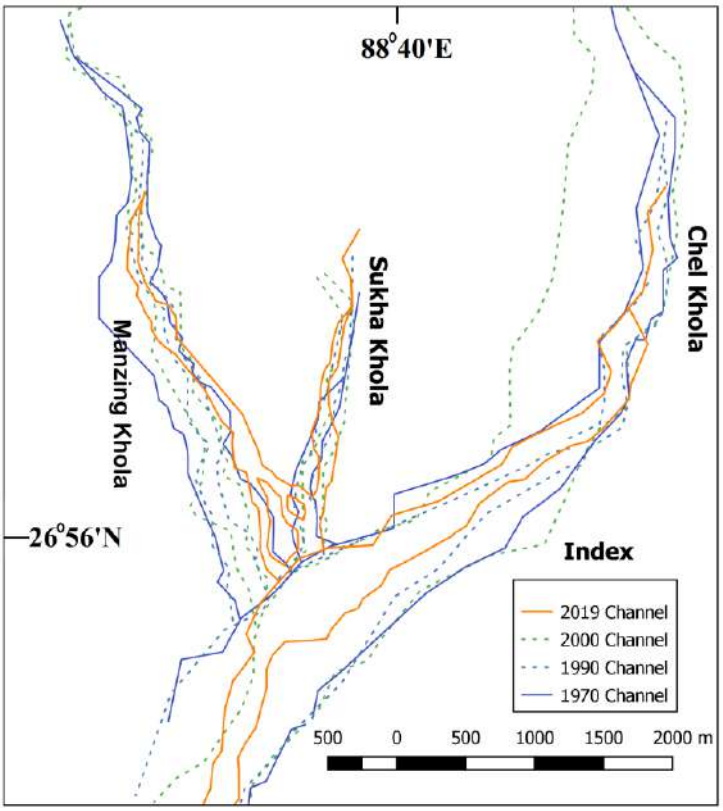

Figure 4.16b Temporal course shifting analysis from satellite images on piedmont surface.

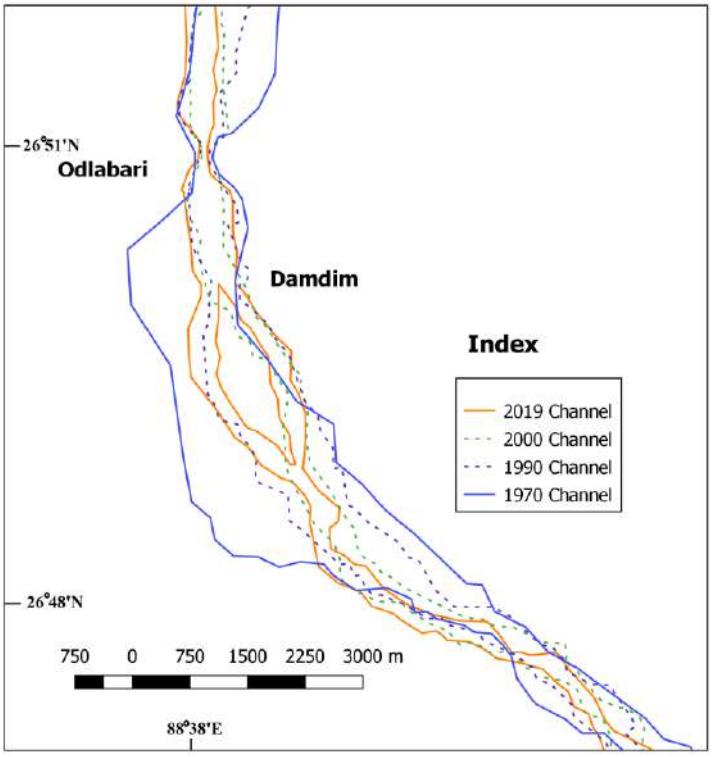

Figure 4.16c Temporal course shifting analysis of lower course of Chel from satellite images.

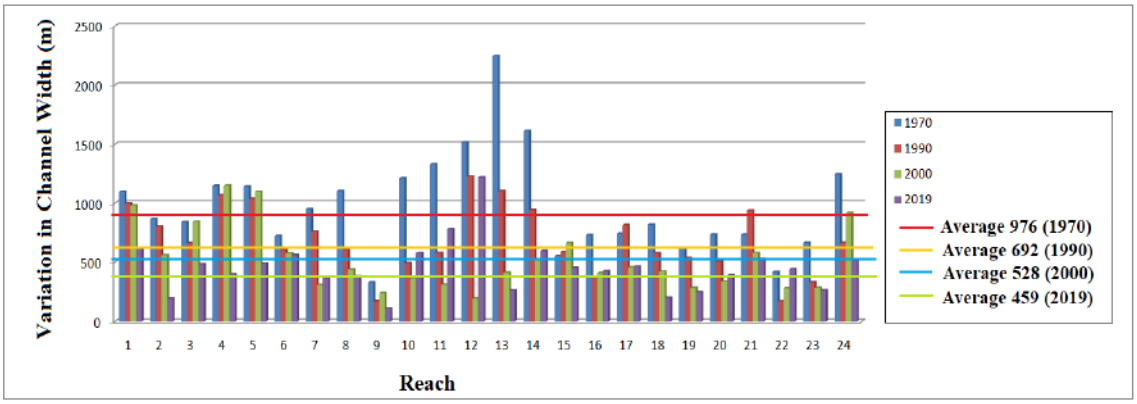

Figure 4.17 Temporal variation of channel width from up to downstream (1 km interval).

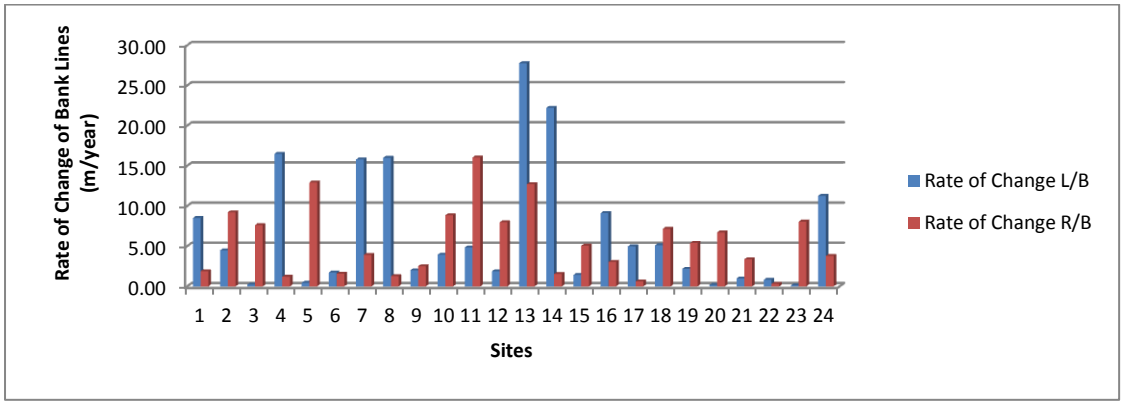

Figure 4.18 Temporal variation in the rate of bank line changes (1970 to 2019).

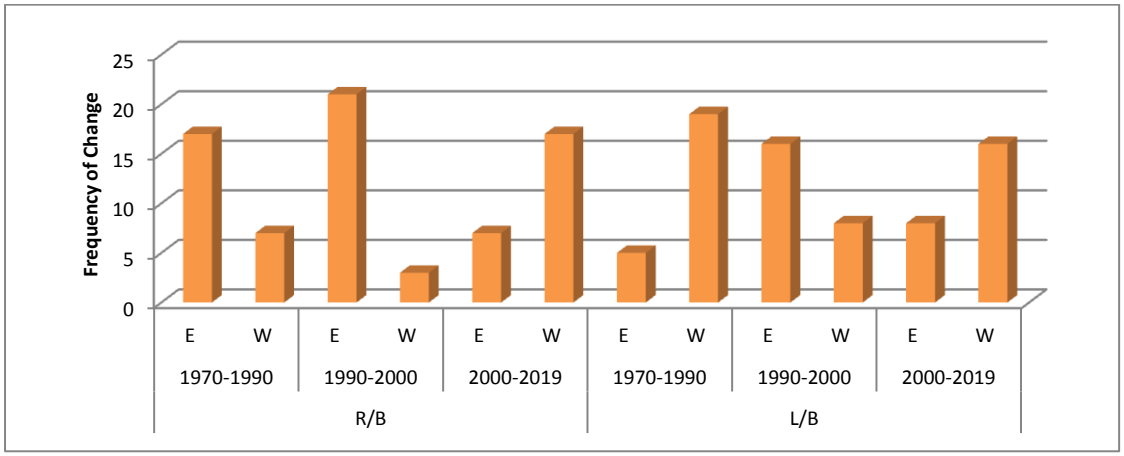

Figure 4.19 Temporal variation in directional changes of banklines.

The average change of left bank (1970 to 2019) has been measured as 331.91 m and the average change of right bank is measured as 271.16 m. The rate of average change of left and right banks are 6.77 m year^{-1} and 5.53 m year^{-1} respectively. The site 13 and 14 indicate maximum change in both bank lines (Fig. 4.18). In directional

analysis, the east-ward chage of the right bank dominates for 1970-1990 and 1990-2000 but the bank line shift direction reversed in 2000-2019. In case of the left bank, the west-ward change dominates in 1970-1990 and 2000-2019 (Fig. 4.19). The randon variability in bank line change indicates the process of active fluvial dynamics and process-form adjustment in the channel since 1970.

4.7 Analysis of channel sinuosity

A channel pattern is considered as a two-dimension, a planform configuration only, regardless of any other floodplain characteristics (Makaske, 2001). The planform geometry of a river can be discussed in to two ways i.e. the single-thread channel pattern and multi-thread pattern. The sedimentary deposits are also helpful in classifying the channel plan forms. In case of multi-thread channel pattern with alluvial fan formation at the mountain outlet probably composed of the bed-load type (Schumn, 1963). The course of Chel up to *Manabari* tea garden (from mountain outlet) exhibits a multi-thread pattern with the formation of many anabranches. But, below *Odlabari* it takes a sharp bend to the S-E. The bend of a channel is inter-connected with its own sediment deposition and transportation type. The bank margins and its composition are always holds a shear strength against the flow types of the channel. The sinuosity depends on the overall soil composition of the floodplain and the gradient along the channel.

The measured sinuosity index value (P = Actual Length/ Straight Length) of Chel river is measured as 1.34 (Muller, 1968). It can also be calculated by dividing the length of a reach as measured along the channel by the length of a reach measured along the valley (Muller, 1968). The major advantage of Muller's calculation is that it measures the amount of deviation of a course from its actual straight line due to causative hydraulic factors and topographic interference (Ezizshi, 1999 and Ghosh et al., 2012). But, the calculated value of standard sinuosity index (1.54) indicates the meandering course of the Chel (Morisawa, 1985). Brice (1964) introduced the sinuosity index defined as the ratio of the channel length to the length of the meander-belt axis. The sinuosity of meandering channel is calculated as the ratio of thalweg length to the air distance (Ezizshi, 1990). The Here, the sinuosity index value of 1.3 is taken as the boundary condition between straight and meandering channel. For a given channel reach, the sinuosity index will generally be lower than the sinuosity

(*P*= distance along the channel divided by straight line distance), for which 1.5 is usually accepted as a boundary value between meandering and straight (Leopold and Wolman, 1957, Rust, 1978, Makaske, 2001).

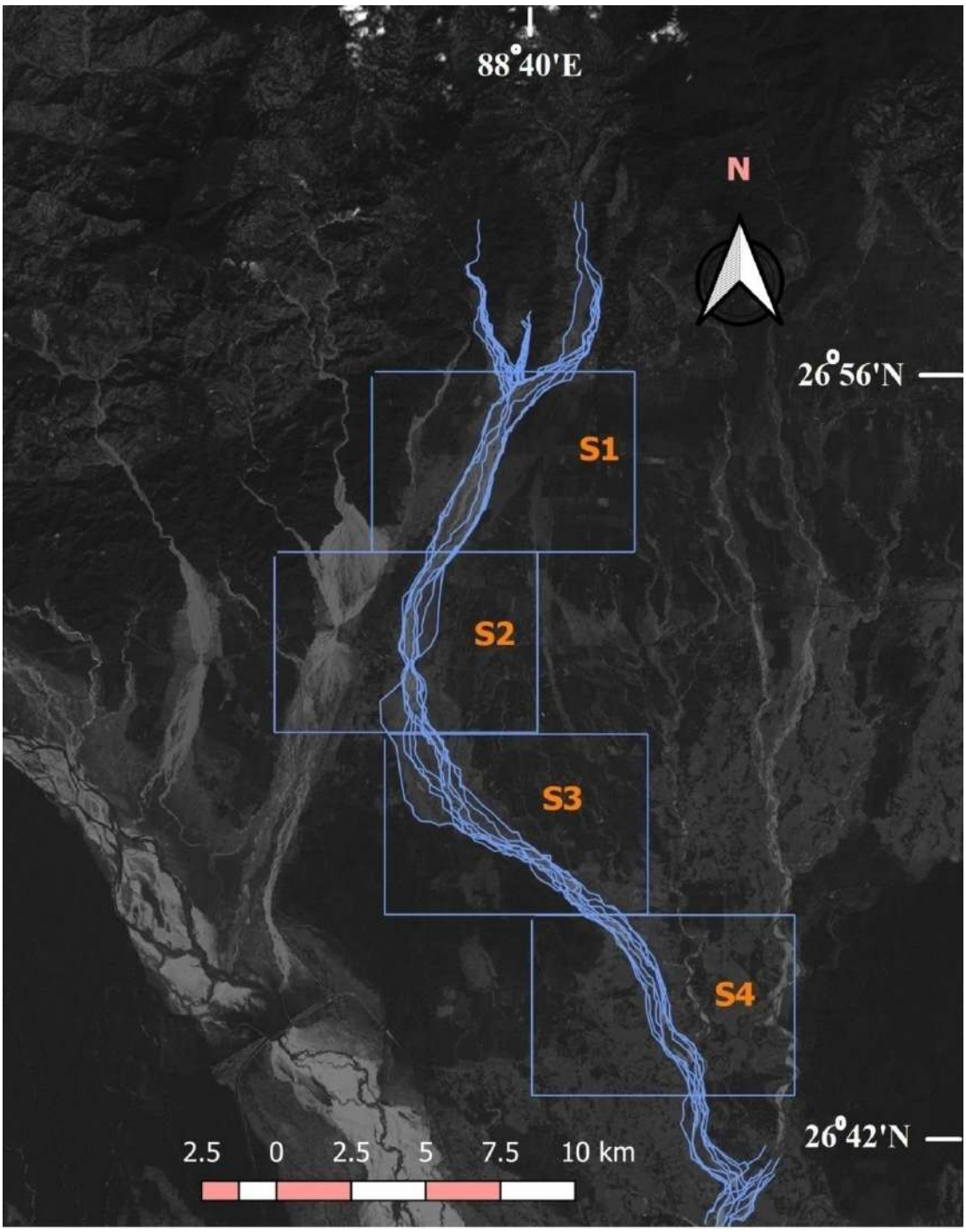

Figure 4.20 Reach design for channel sinuosity analysis.

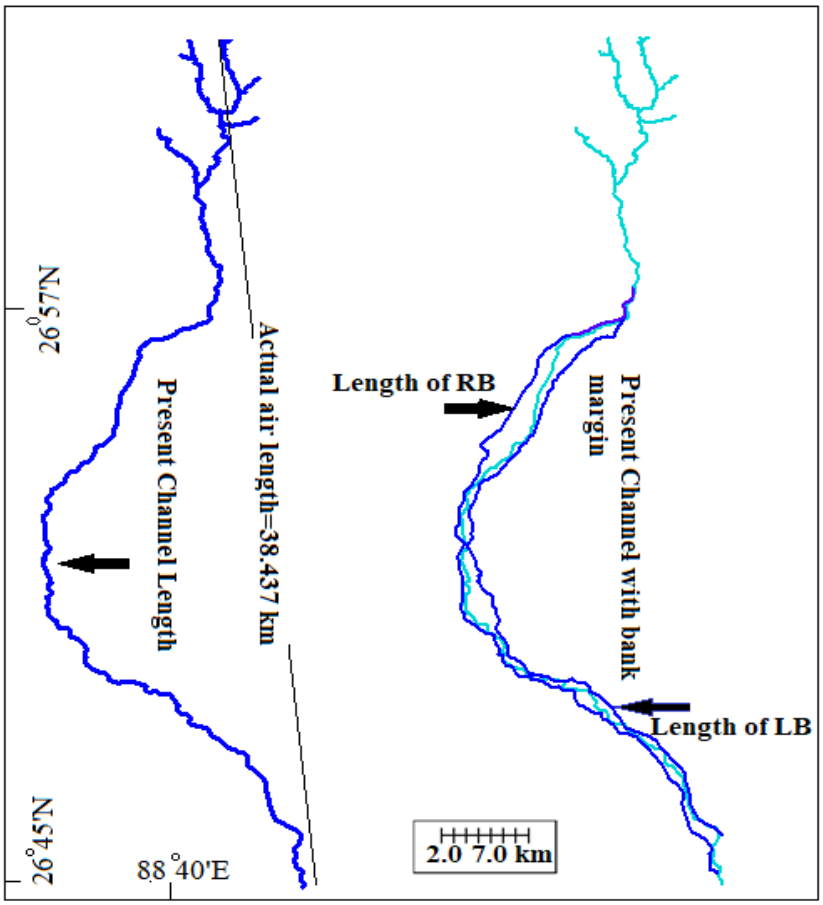

Figure 4.21 Model for the analysis of channel sinuosity.

The channel planform between straight and meandering is called as sinuous (Morisawa, 1985). The channel sinuosity is found in inverse relation to the sediment load at a constant valley slope (Schumn, 1963). The study of sinuosity index of a channel helps us in evaluating the effect of terrain over river course (Panda and Bora, 1992). The measurement of sinuosity index reveals the actual deviation of the straight channel path of a river course (Fig. 4.21). It is related with the valley-wall confinement, composition of bank materials, discharge through the channel and the amount of sediment load passing through a reach.

Table 4.1 Calculation of Sinuosity Index values of 2016 Channel

Reach	CL	VL	AL	CI	VI	HSI	TSI	SSI
R_1	8.30	8.05	7.40	1.12	1.09	33.33	75.00	1.027
R_2	8.20	7.80	7.10	1.15	1.10	50.00	66.67	1.045
R_3	10.32	10.17	9.57	1.08	1.06	33.34	75.00	1.018
R_4	8.20	7.90	7.40	1.10	1.07	42.86	70.00	1.028

Source: Calculated by the author. (Ref. Fig.4.20)

Mueller's (1968) calculation adds an additional site of measuring sinuosity on the basis of the associated topography and hydraulic characteristics of the basin (Table 4.2 & 4.3). The channel's hydraulic sinuosity is not associated with the valley wall confinement (Ghosh et al., 2012).

Table 4.2 Calculation of Sinuosity Index values of 1981 Channel

Reach	CL	VL	AL	CI	VI	HSI	TSI	SSI
R_1	7.64	7.35	6.61	1.16	1.11	4.5	68.75	1.05
R_2	9.89	9.01	8.34	1.19	1.08	1.4	42.10	1.10
R_3	9.13	8.39	8.01	1.14	1.05	1.8	35.71	1.09
R_4	9.17	8.31	8.10	1.13	1.03	3.3	23.08	1.04

Source: Calculated by the author. (Ref. Fig.4.20)

(Note: CL- Channel Length, VL-Valley length, Air Length- Aerial distance between the source and the mouth, Channel Index (Cl)= CL/AL. Valley Index (V.I) = VL/AL, Hydraulic Sinuosity Index (HSI) = % equivalent of CI-VI/VI-1, Topographic Sinuosity Index (TSI) = % equivalent of VI-1/CI-1, Standard sinuosity Index (SSI) = CI/VI.)

It depends on the discharge of water and sediment through a reach. But, the topographic sinuosity is related with the geometry of the valley walls. Here, the channel has been divided into four reaches to derive the values of topographic and hydraulic sinuosity indices. The *hydraulic sinuosity index* (HSI) is the valuable morphometric tools in determining the stage of basin development (Ghosh et al., 2012). The standard sinuosity index calculated maximum (1.11) for the reach 4 (below Apalchad forest) and the course is sinuous (>1.05, Morisawa, 1985). The hydraulic factors are responsible for the sinuosity of this site. The bank wall is mainly composed of cohesive clay, silt and fine sand. The seasonal alterations of channel thalweg cause differential stress on the banks at various places. It leads to promote the differential bank erosion along the channel and changes the shape of the bank lines. The reach 1 (below *Ambiok* TG) is confined by steep valley walls and terraces causes to increase the value of Topographic Sinuosity Index (96.3). The reach 2 (beside *Patharjhora*) is also experienced to get high TSI value (90.00) as because of the presence of old multi-cyclic terrace and coverage of *Mal* forest on the left bank of Chel. The value of HSI at reaches 2 and 3 (R_3, below *Patharjhora* up to the *Odlabari* bridge site) is less because of the channel confinement by embankment (Fig. 4.22). It means that the valley is comparatively constricted as well as the area might have faced rejuvenation.

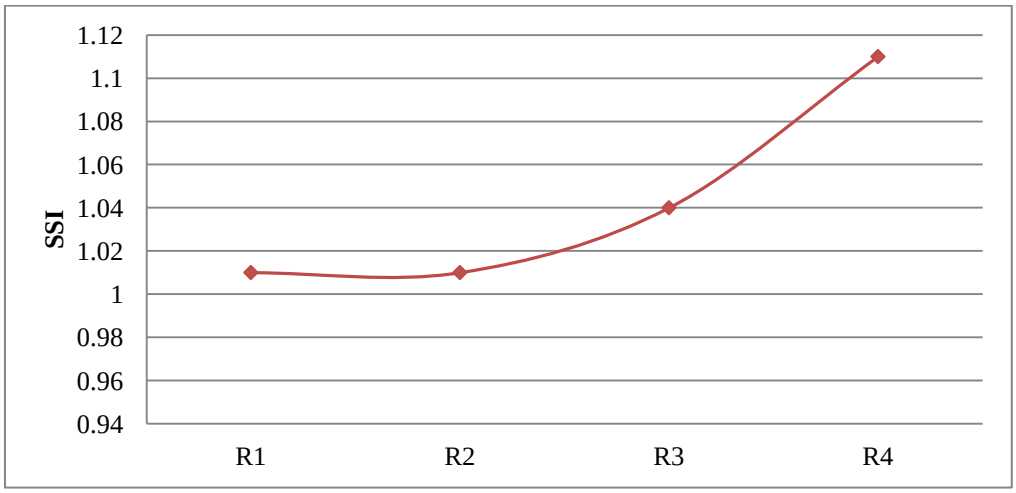

Figure 4.22 Reach wise variation in Standard Sinuosity Index (2016).

The Standard Sinuosity Index (SSI) of the channel increases to the downstream due to the gradual flattening of slope and high amount of bank erosion. The relative increase in SSI indicates the decrease in hydraulic gradient. The reach 4 has revealed minimum effect of topography on the channel sinuosity (Table 4.2).The lower reach (from *Apalchad* to *Rajadanga*) of Chel has been influenced by the left bank tributary of *Mal* river. It causes gradual widening of the channel through bank erosion. The channel flows over the soft alluvium of Chel fan. The channel bank is confined by multi-cyclic terraces and levee depositions. It increases the Topographic Sinuosity value (TSI) of the channel up to reach 3. Below the *Odlabari* bridge, the channel becomes heavily confined by the construction embankment, channel deflectors etc. This anthropogenic constructions lead to increase the value of TSI.

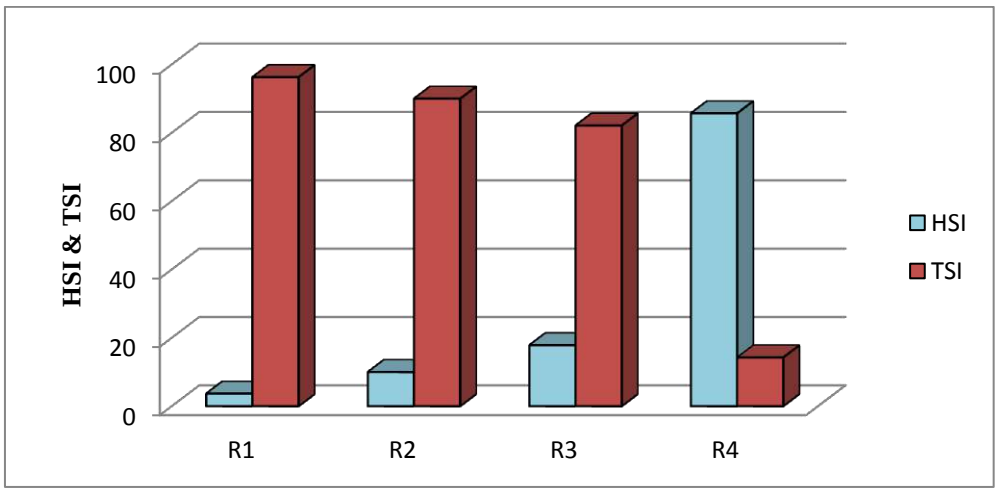

Figure 4.23 Variation in Hydraulic & Topographic Sinuosity Index (2016).

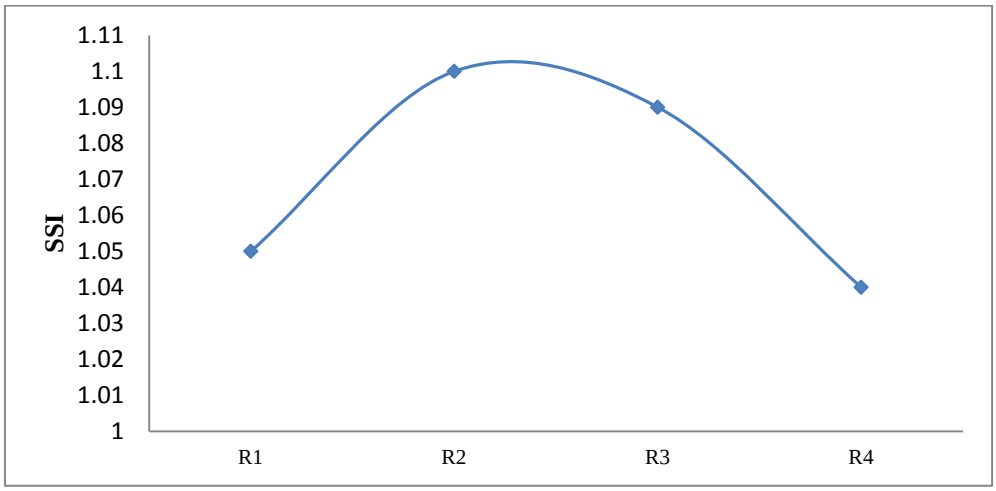

Figure 4.24 Reach (R1-R4) wise variation in Standard Sinuosity Index (1981).

In 1981, the trend of SSI values reveals to form peak at the middle (Fig: 4.24). The reach 2 (between *Patharjhora* and *Odlabari*) expressed high value of SSI (1.10) due to effect of the ongoing process of channel avulsion. The decreasing value of SSI (1.09) in reach 3 is because of the diversion of the channel in to two parts after get retarded by the appearance of a mid-channel bar. The low value of SSI indicates the gradual flattening of the slope by the active hydraulic actions. In 1981, the channel expresses the continuous increase of hydraulic action to the down-stream segment (Fig. 4.24). The channel in reach 1 is affected by the valley wall confinement. The alterations of Channel SSI values express the dynamism of the channel in favour of discharge, bank erosion, bank height, bank composition, effect of channel bars and type of the flood plain. Within a span of 36 years, the shape of the channel on the basis of sinuosity analysis has been completely changed with changing fluvial activities in the channel. The present course of Chel attends quasi-stability below *Patharjhora* up to the confluence with Mal river. The main channel is flowing on the foreland basin and it gradually filling it up with the competent flow up to the Apalchad forest. The channel filling causes the appearance of some permanent bars and seasonal bars. The alterations of bar formation are basically confined at the up-stream of *Odlabari* bridge. The down-stream part has continuously been matured by the formation of stable bars. As the channel progresses in the cycle of erosion, the role of the hydraulic sinuosity increases over the Topographic Sinuosity. The nature of braiding and channel sinuosity has its reciprocal relationship in determining the dynamic nature of the channel slope.

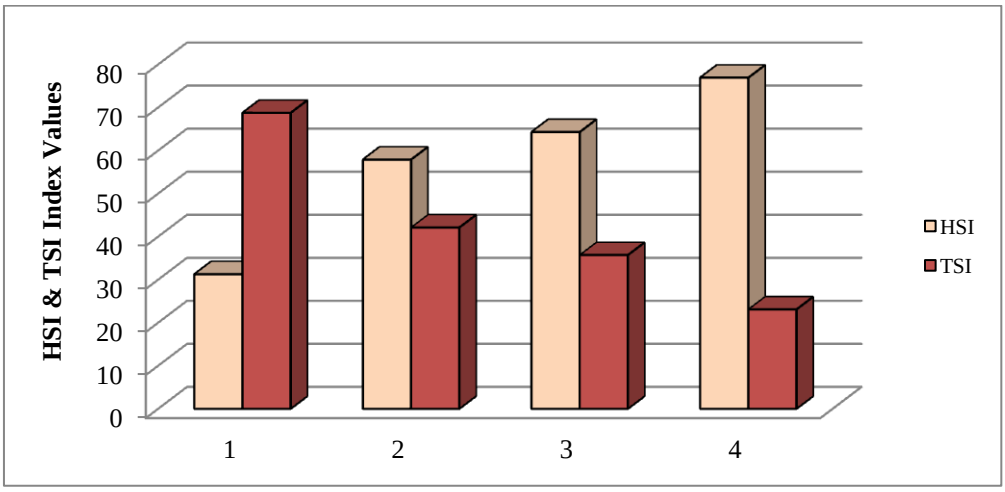

Figure 4.25 Variation in Topographic & Hydraulic Sinuosity Index (1981).

4.8 Analysis of Braiding parameters

The pattern of a channel is related with the amount of sediment delivery in the channel, transportation of the sediment and various parameters of controlling channel geometry. Sediment transportation and low threshold of bank erosion are the essential conditions of braiding (Leopold et al., 1964). The alluvial channels on the piedmont are mostly dominated by bed-load infested courses. Such courses further develop braided channel patterns. Braided patterns display the scaling hierarchy of channel sizes (Rust, 1978). Braiding is a type of channel adjustment that may be made in a channel possessing a particular bank material in response to a debris load too large to be carried by a single channel (Leopold et al., 1964). Brice (1964) developed the way of calculating Braiding Index as a measure of the total amount of bank length where most islands or bars have a significantly greater than the width (Friend et al., 1993). In the calculation, the total bank length can be approximated by doubling the islands or bar lengths. The calculation follows the formula Braiding Index (BI**)** = 2* Summation of all islands and bars in the reach/ Length of the reach measured mid-way between banks of the channel belt.

Rust (1978) modified that channel thalwegs be used to define a braid length from up-stream divergence to the down-stream convergence. Friend and Sinha (1993) investigated on the existing processes of braiding index calculation and found out Braid-Channel ratio. It is a ratio between the mid-channel lengths of primary channels and the widest channel in the reach.

Table 4.3 Computations on Braiding & Sinuosity Indices

Reach No	$\sum L_b$	L_m (Km)	P	P_{ctot}	$B=P_{ctot}/P$ (Friend & Sinha, 1993)	Richards (1982) $B=L_{cot}/L_{cmax}$	Rust (1978) $B_P=\sum L_b/L_m$	Brice (1964) BI	SI	Composite BI & SI (BI+SI)	Gradient (1: HE /VI) m/m
1	11.4	1.2	1.01	11.02	10.91	10.9	9.5	4.0	1.01	5.01	0.06
2	9.17	0.74	1.11	11.42	10.28	10.3	12.3	7.6	1.11	8.71	0.07
3	9.30	1.01	1.01	7.12	7.04	7.05	9.2	9.04	1.01	10.05	0.11
4	10.01	1.13	1.02	6.15	6.03	6.0	8.8	6.54	1.02	7.56	0.16
5	5.20	1.08	1.05	5.8	5.52	5.5	4.8	4.46	1.05	5.51	0.15
6	9.37	1.16	1.10	7.02	6.38	6.4	8.0	3.69	1.10	4.79	0.36
7	17.80	2.0	1.20	8.9	7.42	7.4	8.9	6.36	1.20	7.56	0.32
8	12.31	1.76	1.11	6.85	6.17	6.9	6.9	4.5	1.11	5.61	0.36
9	16.5	3.2	1.12	5.3	4.73	4.7	5.1	4.84	1.12	5.96	0.26
Range						4.7 – 10.9	5.1-12.3				
Median						6.9	8.8				
Mean						7.24	8.17				
Skewness						0.955	0.073				

Source: Computed by the authors.

Note: $\sum L_b$- Sum of braid channel lengths, L_m- the mean of the meander wavelengths in a reach of the channel belt, P- Sinuosity parameter, P_{ctot} or L_{cot} - Sum of the mid channel lengths of all segments of primary channels, L_{cmax}- Mid channel length of the widest channel, B- Braid-Channel Ratio, B_P-Braid Parameter, BI- Braid Index, SI- Sinuosity Index, HE- Horizontal distance (Contour segment) & VI- Vertical Interval (Contour segment).

4.9 Relationship of Braid and Sinuosity parameters

The total sinuosity of a river is a combined measure of channel sinuosity and degree of braiding. The correlation of channel braiding and sinuosity for the selected reaches result into moderate positive correlation with value of r = 0.69. The braided index is able to explain (R^2 0.48) 48% variables of the values of Sinuosity Index. The relationship between braiding and Sinuosity Index is showing a positive trend that change in one variable with causal change in the other. Hence braiding can be explained as positive impetus to sinuosity. The relation in power equation results the R^2 of 0.42 compared to R^2 of exponential equation of only 0.37 and R^2 of linear equation is 0.35 i.e. a difference of 0.02 being nominal in validity. Maximum R^2 has been noticed in case of polynomial ($y=-0.021x^2+0.322x-0.209$) relations i.e.0.48 and higher trends of braiding is associated with maximum number of bars (Fig. 4.26). But, it is very hard to say about the persistence of positive trend of sinuosity and braid relation at various reaches to downstream because, seasonal hydrodynamics of the channel frequently changes the nature of bar deposition within the channel. So, the braiding causes minimum influence on channel sinuosity in case of Chel. But, the process of channel avulsion is mainly controlling the channel sinuosity on the

piedmont zone. But the lower part of the channel below *Odlabari,* the channel sinuosity is the manifestation of bar formation and increasing near bank stress which causes the bank failure during monsoon.

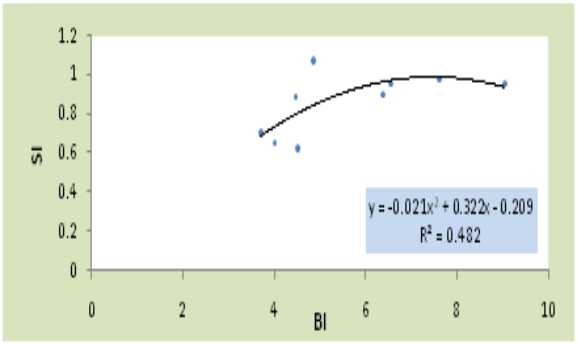

Figure 4.26 Regression between Braided Index (BI) & Sinuosity Index (SI).

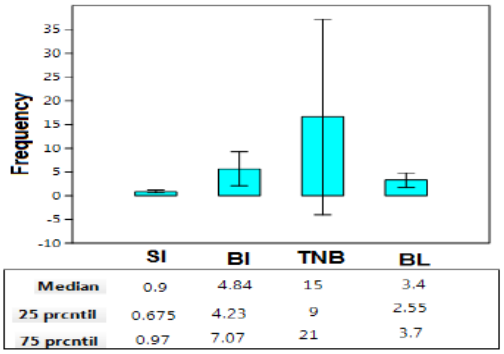

Figure 4.27 Whisker plot of relational statistics.

Note: SI-Sinuosity Index, BI-Braid Index, TNB-Total No. of Bars, BL-Bar Lengths (m).

4.10 Conclusion

The channel of Chel indicates a high and complex braided pattern in the piedmont surface. The channel behavior reflects its tendency of auto-cyclic cut and fills processes related to recent base level changes. The heterogeneity of load and nature of dispersal over the alluvial fan surface prepares the essential condition like the case of braiding of river Chel having been adjusted with the dynamic nature of auto-cyclic processes of cut and fill. More over a complex or volatility of braid vs. sinuosity has been noticed in case of the river which unshadows no spectacular trend over time. The channel exhibits succession of fan sediment that indicates the maturity of the surface with channel braided network triggered by flood recurrences. Sediment transportation and low threshold of bank erosion are the essential conditions of braiding. On the piedmont surface, the competent flow of the channel bears the affinity to processes of avulsion and hydraulic friction to cut across the thalweg along the course. But, the submerged coarse particles scroll over the bed until the flow losses its competency. The variability of channel's maximum depth brings irregularities in D-W ratio (Depth-Width Ratio). The maximum depths in 2017 in pre & post monsoon conditions increase the D-W ratio (0.018) and lead to increase network circuits and connectivity. Moreover the channel with its head waters are sensitive to haphazard

bed stagnancy and differential flow patterns resulting into enhanced chances of braiding.

Plate 4.1 Course of chel at the end of hilly tract below Upper Fagu (2015).

Plate 4.2 Up-stream braided course of Chel at Odlabari (2015).

Plate 4.3 Channel with heterogeneous bed load at Patharjhora (2015).

Plate 4.4 Semi-braided course of Chel at Rajadanga (2015).

4.11 References & Bibliography

Acharyya, S.K., (1980), Structural Framework and Tectonic evolution of the eastern Himalaya, Himalayan Geology 10, pp. 412-439.

Allen, J.R.L., (1965), A review of the origin and characteristics of recent alluvial sediments, Sedimentology 5 (2), pp. 89–191.

Ashmore, P. E., (1991), How do gravel-bed Rivers braid?. *Canadian Journal of Earth Sciences*, 28, 326–341.

Bagnold, R.A., (1954), Experiments on a Gravity free dispersion of large solid sphere in a Newtonian fluid under Shear Stress, Royal society of London, Proc., Ser. A, Vol. 225, pp.174-205.

Bansal, B. K. and Verma, M., (2013), Active fault research in India: achievements and future perspective. *Geomatics, Natural Hazards and Risk*. 7(01), Taylor and Francis Group, pp. 65–84(73).

Brice, J.C., (1964), Channel Patterns and Terraces of the Loup Rivers in Nebraska, Geological Survey Professional Paper 422D, Washington, pp. D2-D41.

Carson, M.A., Griffiths, G.A., (1987), Bedload transport in gravel channels. New Zealand Jr. Hydrol., 26(1), 1–115.

Chakraborty, T & Ghosh, P, (2015), The Geomorphology and Sedimentology of the Tista megafan, Darjeeling Himalaya: Implications for megafan building processes, Geomorphology 115, Elsevier Publication, pp.252-256.

Charlton, R., (2008), Fundamental of Fluvial Geomorphology, Taylor & Francis Library, ISBN 0-203-37108-9, pp. 129, 145.

Cheng-Wei, K., Chi-Farn, C., Su-Chin, C., Tun-Chi, Y. & Chun-Wei, C., (2017), Channel planform dynamics monitoring and channel stability assessment in two sediment-rich Rivers in Taiwan MDPI, *Water*, 9 (84) doi: 10.3390/w9020084, pp.1-16(1).

Ezizshi, A.C., (1999), An Appraisal of the existing Descriptive measures of River Channel Patterns, Journal of Environmental Sciences, Vol. 3(2), pp. 253-257.

Ferguson, R,I. (1993), Understanding Braiding Processes in Gravel Bed Rivers, Progress and Unsolved problems, in J.L. Best & C.S. Bristow (eds.), Braided Rivers, Special publication of the Geological society of London 75, pp. 73-87.

Friend, F P and Sinha, R, (1993). Braiding and meandering parameters. *Geological Society*, London, Special Publications, 75, pp.105-111.

Ghosh, S. & Mistri, B., (2012), Hydro-geomorphic Significance of Sinuosity Index in relation to River Instability: A case study of Damodar River, International Journal of Advances in Earth Sciences, Vol.01, Issue 2, pp.50 & 51.

Guha, D., Bardhan, S., Basir, S.R., De, A.K., Sankar, A., (2007), Imprints of Himalayan thrust tectonics on the Quaternary piedmont sediments of the Neora-Jaldhaka Valley, Darjeeling Sikkim Sub-Himalayas, India, *Journal of Asian Earth Sci*., 30, pp.464–473.

Järvelä, J., (2004), Flow resistance in environmental channels: focus on vegetation. Helsinki University of Technology Water Resources Publications, Teknillisen korkeakoulun vesitalouden ja vesirakennuksen julkaisuja, Espoo 2004 , TKK – VTR - 10, Dissert., D.Sc. (Technology), Department of Civil and Environmental Engineering (debate in Auditorium R1 at Helsinki University of Technology), pp.1-54 (9 &10).

Jhon, F., (2000), Channel Avulsion on Alluvial fans in Southern Arizona, Geomorphology 37, Elsevier Publication, pp. 99-101.

Jones, H.L. & Hajek, E.A., (2007), Characterizing Avulsion Stratigraphy in ancient Alluvial deposits, Sediment Geology, 202, Elsevier Publication, pp.125, 134, and 135.

Kansky K., (1963), Structure of Transportation Networks: Relationships Between Network Geometry and Regional Characteristics PhD thesis, RP84, Department of Geography, University of Chicago Kissling C, 1969, ``Linkage importance in a regional highway network" The Canadian Geographer 13(2), pp.113-127.

Leopold, L. B. & Wolman, M. G., (1957). River channel patterns –braided, meandering and straight. *Professional Paper of the US Geological Survey*, 282 B, 46, 49 & 53.

Leopold, L.B. and Wolman, M.G. (1957), River Channel Patterns, Braided, Meandering and Straight. U.S. Geol. Surv. Paper. 282-B.

Leopold, L.B. Wolman, G. and Miller J.P., (1964), Fluvial processes in geomorphology, Dover Publications Inc., New York, pp. 180, 282, 284, 292, 294, 295.

Makaske, B. (2001), Anastomosing Rivers: A review of their Classification, origin and sedimentary products, Earth Science Review 53, pp. 96-149.

Mollard, J. D., (1973), Airphoto interpretation of fluvial features. Edmonton, A. *Proceedings of the 9th Canadian Hydrology Symposium*, *Canada: NRCC (National Research Council of Canada)*, pp.341 – 380.

Morisawa, M. (1968), Streams- Their Dynamics and Morphology, McGraw-Hill Book Company, London, pp.37, 51, 52

Morisawa, M. (1985), River - Forms and Process. Longman, London.

Muller, J.R., (1968), An Introduction to the Hydraulic and Topographic Sinuosity Indexes, Annals of American geographers, Vol. 58, No.02, pp.371-385.

Nanson, G. C., Huang, H. Q., (1999), Anabranching Rivers: divided efficiency leading to fluvial diversity. In: Miller, A J, Gupta, A (Eds.), Varieties of Fluvial Form. Wiley, Chichester, pp. 477 – 494.

Nanson, G. C., Huang, H. Q., (1999), Anabranching Rivers: divided efficiency leading to fluvial diversity. In: Miller, A J, Gupta, A (Eds.), *Varieties of Fluvial Form*. Wiley, Chichester, pp.477 – 494.

Nanson, G.C. & Knighton, A.D., (1996), Anabranching Rivers: Their Cause, Character, Classification, Earth Surface Processes, Land-Forms 21, pp.39-217.

Panda, P.C. & Bora, H.N., (1992), A study on Sinuosity Index of Siang River and its major tributaries: Arunachal Pradesh, in Rai, R.K., Mahapatra, A.C. and Goel, N.D. (eds.), Environmental Management: Physio-ecological facets, Vol. 01, Rawat Publications, New Delhi, pp. 97-102.

Rust, B R, 1978. A classification of alluvial channel systems. *CSPG (Canadian Society of Petroleum Geologists)*, Memoir, 5, pp.187-198 (188).

Schumn, S.A., (1963), Sinuosity of Alluvial Rivers on the Great Plains, Bull. Geological society of America, Vol. 74, pp. 1089-1100.

Slingerland, R & Smith, D.N., (2004), River Avulsions and their deposits, Annual Rev. Earth Planet Sci. 32, DOI 10.1146/annurev.earth.32.101802.120.210, pp. 261-265.

Smith, N.D., 1970. The braided stream depositional environment; comparison of the Platte River with some Silurian clastic rocks, N. Central Appalachians. *Bull. Geol. Soc. Am.*, 81, pp. 2993–3014.

Srivastava, V., Mukul, M., (2017). Quaternary deformation in the Gorubathan recess: Insights on the structural and landscape evolution in the frontal Darjiling Himalaya. *Quaternary International, ELSEVIER*, 462, p.139.

Starkel, L. , Sarkar, S., Soja, R., Prokop, P., (2008), Present Day Evolution of the Sikkimese-Bhutanese Himalayan Piedmont, Instytut Georafii Przestrzennego, Poland, PLISSN 0373-6547, ISBN 978-83-61590-09-5, pp. 53, 54, 62.

Starkel, L., Płoskonka, D., Adamiec, A., (2015), Reconstruction of late quaternary neotectonic movements and fluvial activity in sikkimese-bhutanese Himalayan piedmont. *Studia Geomorphologica Carpathian – Balcanica*, XLIX, PL ISSN 0081-6434, pp.71–82.

Wiejaczka, L, (2016), Riverbeds level changes in the margin and foreland of the Darjeeling Himalaya during the years with a normal Monsoon Rainfall, Springer's Japan, R.B. Singh & P. Prokop (eds.), Environmental Geography of South Asia, Advances in Geographical and Environmental Sciences, DOI. 10.1007/978-4-431-55741-85, p.85.